12-8-2017

Efficacy of Novel Pyridinium Oximes in Preventing Neural Damage

Charles Andrew Leach

Efficacy of novel pyridinium oximes in preventing neural damage

By

Charles Andrew Leach

A Thesis
Submitted to the Faculty of
Mississippi State University
in Partial Fulfillment of the Requirements
for the Degree of Master of Science
in Environmental Toxicology
in the College of Veterinary Medicine

Mississippi State, Mississippi

December 2017

Efficacy of novel pyridinium oximes in preventing neural damage

By

Charles Andrew Leach

Approved:

_____

Janice E. Chambers
(Major Professor)

_____

Russell L. Carr
(Committee Member/Graduate Coordinator)

_____

Alicia K. Olivier
(Committee Member)

_____

Mark L. Lawrence
Associate Dean
College of Veterinary Medicine

Name: Charles Andrew Leach

Date of Degree: December 8, 2017

Institution: Mississippi State University

Major Field: Environmental Toxicology

Major Professor: Dr. Janice E. Chambers

Title of Study: Efficacy of novel pyridinium oximes in preventing neural damage

Pages in Study 77

Candidate for Degree of Master of Science

Organophosphates are neurotoxic compounds that inhibit acetylcholinesterase producing excess cholinergic stimulation. This produces various toxic signs including excitotoxic neuronal damage. Oximes can be used as a treatment for organophosphate poisoning by reactivating inhibited acetylcholinesterase. Traditional oximes do not penetrate the blood-brain barrier, limiting protection of the central nervous system. Novel, brain-penetrating oximes have the potential to protect the brain from organophosphate induced damage. Adult male rats were used to examine the ability of model organophosphates to produce neuropathology and the ability of novel oximes to prevent this damage. Additionally, adult male rats were used to examine changes in gene expression of the MAP kinase system resultant of treatment with model organophosphates and novel oximes. Results of these experiments support that the model organophosphates can be used to study neurodegeneration, the novel oximes may prevent neurodegeneration, and both organophosphates and novel oximes affect expression of MAP kinase genes.

DEDICATION

This thesis is dedicated to my family, who have always shown me unconditional love and supported me in all of my endeavors, and especially to my wife Angela who has been with me through this process.

ACKNOWLEDGEMENTS

I would like to thank the members of my thesis committee, Dr. Jan Chambers, Dr. Russell Carr, and Dr. Alicia Olivier, for their help and support during this project. I would also like to acknowledge Dr. Jeff Eells and Dr. Tim Morgan for their contributions to my understanding of the underlying physiology of the research described here.

I would like to thank Dr. Ron Pringle and Mary Beth Dail for their companionship and help and training in the methods used in this project. I would like to thank Edward Meek and Shane Bennett for all of the work that they put into animal treatments and sample preparation for this project. I thank Erle Chenney for his help in assays associated with this project. I would also like to thank Dr. Trey Howell, Dr. Robert Wills, Shirley Guo-Ross, and John Stokes for advice regarding various methods used in this study.

I would like to thank my fellow graduate students, Steve Dezell, Royce Nichols, Sandeep Kondakala, Navatha Alugubelly, Afzaal Mohammad, Antonio Ward, and Jason Garcia, for their companionship during my time in this program.

This Research was supported by the CounterACT program of the National Institute of Neurological Disorders and Stroke of the National Institutes of Health under Award Number U01NS083430.

TABLE OF CONTENTS

LIST OF TABLES

LIST OF FIGURES

ABBREVIATIONS

2-PAM	Pralidoxime
ACh	Acetylcholine
AChE	Acetylcholinesterase
AP-1	Activating protein-1
ATF-2	Activating transcription factor 2
BBB	Blood-brain barrier
BDNF	Brain-derived neurotrophic factor
BuChE	Butyrylcholinesterase
CaMKII	Calcium/calmodulin-dependent protein kinase II
CNS	Central nervous system
CNTF	Ciliary neurotrophic factor
CWA	Chemical warfare agent
ERK	Extracellular regulated protein kinase
FGF-2	Fibroblast growth factor
GFAP	Glial fibrillary acidic protein
HSP72	Heat shock protein 72
IL1β	Interleukin 1β
IL6	Interleukin 6

JNK	c-Jun N-terminal kinase
MAPKK	MAP kinase kinase
MAPKKK	MAP kinase kinase kinase
MEF2	Myocyte enhancer factor 2
MEK	MAP/ERK kinase
MEKK	MAP/ERK kinase kinase
NEMP	Nitrophenyl ethyl methyl phosphonate
NGF	Nerve growth factor
NIMP	Nitrophenyl isopropyl methyl phosphonate
OP	Organophosphate
PLC γ	Phospholipase C γ
PON-1	Paraoxonase-1
Pxn	Paraoxon
qPCR	Quantitative polymerase chain reaction
TNFα	Tumor necrosis factor α
TNTC	Too numerous to count
VEGF	Vascular endothelial growth factor

CHAPTER I

INTRODUCTION

1.1 Brief History of Organophosphates

Organophosphates (OPs) consist of a diverse group of compounds having a variety of uses including: pesticides, fire retardants, plasticizers, and chemical warfare agents (CWAs). The first documented synthesis of an organophosphate was the creation of methyl phosphor chloride by Von Hoffman in 1837. Several developments by other scientists followed in the following years, but the most notable occurred in 1934 when the German chemist Gerhard Schrader was tasked with developing pesticides. His group developed roughly 2000 different compounds including parathion, tabun, sarin, and soman. While parathion could be used as a pesticide, the toxicities of tabun, sarin, and soman were such that they could not be safely used for this purpose. This toxicity did provide the potential for their use as CWAs. Due to this potential, tabun and sarin were manufactured in a factory outside Duhernfurt, for potential use in the war effort. Following the end of the war, large quantities of these chemicals were seized by the Allies. The chemicals developed by the Germans were given code names beginning with "G" to signify German. Research by Allies scientists after the war produced additional compounds given codes starting with "V" to signify victory. VX (S-2 diisopropylamino O-ethylmethylphosphonothioate) was developed by British scientists in 1952. The Russians produced a similar compound called VR (N, N-diethyl-2-methyl-2-methylpropoxy phosphorylsulfanylethanamine). Other agents in the V series are VE (S-2-

diethylaminoethyl O-ethylethylphophonothioate), VM (2-ethoxy-methylphosphoryl sulfanyl-N, N-diethylethanamine), and VG (2-diethoxyphosphorylsulfanyl-N, N-diethylethanamine). Following WWII, development of OPs as pesticides continued and their popularity only increased after use of organochlorine compounds was banned (Soltaninejad & Shadnia, 2014). In the United States, organophosphates constituted more than 70% of all pesticides used during some years of the 1980s and 1990s. This use has since declined with the advent of newer, less toxic pesticides (U. S. Environmental Protection Agency, 2007).

Despite significant production during World War II, use of organophosphates in warfare did not occur until the Iran-Iraq War (1980-1988). The United Nations confirmed that Iraq used tabun and sarin on both Iranian soldiers and civilians. It is estimated that through multiple deployments of OP and sulfur mustard CWAs, over 100,000 people were poisoned during the Iran-Iraq War. During the First Persian Gulf War, while CWAs were not used, US service members may have been exposed to sarin and cyclosarin following the destruction of Iraqi munitions. OP CWAs have also been used in terrorist attacks such as the release of sarin by Aum Shinrikyo in the Tokyo subway that resulted in 11 deaths and the poisoning of 5500 others. (Soltaninejad & Shadnia, 2014). Most recently, sarin has been deployed in Syria in 2013 and 2017 by the Assad regime resulting in many civilian deaths (Adamson & Vasilyeva, 2017; Loveluck, 2017).

1.2 Properties of Organophosphates

Organophosphates used as pesticides and CWAs are potent anticholinesterases that phosphorylate acetylcholinesterase (AChE) inhibiting its ability to hydrolyze the neurotransmitter acetylcholine (ACh). This leads to an excess of ACh in synapses and neuromuscular junctions. Accumulation of ACh affects nicotinic and muscarinic acetylcholine receptors both in the peripheral and central nervous systems. These supraphysiological levels of cholinergic stimulation produce an array of toxic signs in exposed individuals including: excessive secretions from bronchial, salivary, ocular, and intestinal glands, miosis, bronchospasm, bradycardia, muscle fasciculations, respiratory suppression, seizures, and death (Watson et al., 2009).

ACh is responsible for chemical signal transduction of autonomic neuronal ganglia, parasympathetic innervation of organs, sympathetic innervation of sweat glands, motor innervation of skeletal muscles, and signal conduction between central nervous system (CNS) neurons. It is released from axonic terminals of cholinergic neurons into the synapses following the conductance of an action potential down the axon. It is released from vesicles into the synapse where it interacts with ACh receptors on the post-synaptic membrane transmitting the signal to the target cell. ACh within the synapse is quickly hydrolyzed by AChE to terminate signal transduction. To accomplish hydrolysis, ACh temporarily binds to AChE. The positive charge of the quaternary nitrogen in the choline group electrostatically binds to an anionic site assisted by auxiliary binding of the adjacent methyl groups. Subsequently the carbonyl carbon of acetate covalently binds to the esteratic site of AChE. Following this binding, the ester linkage between acetate and choline is broken and choline leaves the protein. Finally, a reaction between water and

acetate occurs and acetic acid is released returning AChE to its active form (Gallo & Lawryk, 1991).

Organophosphates' effects on AChE result from their esteric structure. B-class esterases such as AChE react with OPs but become persistently phosphylated preventing them from performing their normal actions on other esters such as ACh. The phosphorus atom of the OP binds to the esteratic site and the OP may or may not have a positive charge in the acidic group to interact with the anionic site. The acidic leaving group separates from the rest of the OP, which is left bound to AChE. Where removal of the normal substrate for this enzyme would occur in less than a second, hydrolysis of the bound OP can take more than 1000 hours in some of the more persistent compounds. The time needed for hydrolysis is a function of the compound left attached to AChE and is not affected by the leaving group (Gallo & Lawryk, 1991).

While initially slowly reversible, OPs "age" at a variable rate depending on the compound. Aging is the result of loss of an alkyl or alkoxy group that irreversibly binds the OP to the AChE molecule (Watson et al., 2009). Aging of phosphorylated AChE is most easily observed when a reactivator such as a nucleophilic oxime used to reverse the phosphorylation cannot remove the portion of OPs that are aged. Reactivation of phosphorylated AChE becomes progressively less efficient the longer that the phosphorylation has been present with an increasing amount of the enzyme being completely resistant to reactivation. This aging takes place at an exponential rate. The hydrolysis of an alkyl or alkoxy group leaves a monoalkoxy moiety that cannot be removed by nucleophilic attack. The function of an irreversibly inhibited AChE molecule can only be restored by producing a new molecule of AChE to take its place. This takes

place in different manners in different tissues. Red blood cells lack the ability to synthesize more cholinesterase, so circulating cholinesterase can only be restored through erythropoiesis in the bone marrow. Plasma cholinesterase is restored by the liver. AChE within the brain is synthesized in the neuronal cell body and transported by axonal flow to the synaptic terminals, this being indicated by regeneration of synaptosomal AChE occurring 24 hours after regeneration within the microsomal fraction (Gallo & Lawryk, 1991; Austin & James, 1970).

With the esteratic site occupied, AChE cannot degrade ACh. Continuing release of ACh within the synaptic cleft produces an increased concentration of ACh. Accumulation of ACh produces the majority of the effects seen with organophosphate poisoning. These signs include sweating, miosis, lacrimation, salivation, respiratory tract secretion, vomiting, muscle fasciculations, cardiac arrhythmia, heart block, seizures, and coma. Death can occur within 5 minutes of exposure with high doses of the most toxic OPs. Death due to OP poisoning is generally due to respiratory failure but may result from cardiac failure as well. CNS involvement is not required but can contribute to lethality. Respiratory failure is likely a result of inhibition of the respiratory centers in the brainstem, bronchoconstriction, bronchial secretions, and paralysis of the respiratory muscles (Costa, 2008).

1.3 Therapeutic Intervention

Therapy of OP exposure consists of several components that work through different mechanisms. Should immediate future organophosphate exposure be expected, pretreatment therapies can decrease the severity of OP intoxication. Following exposure, direct anticholinergic treatments can be used to combat the effects of the OP. Finally,

oximes directly target OP molecules bound to AChE to restore its normal function (Masson, 2011).

1.3.1 Pretreatments

Prophylactic pretreatments consist of two general categories, reversible AChE inhibitors that temporarily bind AChE so that it is unavailable for OP binding and bioscavengers that inactivate OP molecules before they are able to react with physiological targets. The reversible AChE pretreatment currently in use is pyridostigmine bromide. It is a carbamate that transiently carbamylates AChE protecting it from phosphorylation. It does not cross the blood-brain barrier (BBB), and therefore provides no CNS protection. Use of pyridostigmine along with exposure to several other stressors has been associated with development of Gulf War Syndrome (Masson, 2011).

The body contains a variety of compounds in its tissues that are able to detoxify OPs and with low exposures may prove almost completely protective. It is also possible that exogenous bioscavengers might be able to be administered for protection against OP exposure. Bioscavengers may be able to react with OP compounds either stoichiometrically or catalytically. Butyrylcholinesterase (BuChE), likely one of the most important endogenous bioscavengers, is present in human plasma at a concentration of about 50 nM. It serves no known biological function and is able to stoichiometrically (1 BuChE: 1 OP molecule) react with OPs in the bloodstream. Limited amounts can be produced for exogenous administration to provide more protection than is normally present in the human bloodstream. There are natural enzymes within the human body that have the potential to act as catalytic bioscavengers of OPs. The most promising of these is paraoxonase-1 (PON-1). It is produced by the liver and is able to hydrolyze some OP

molecules at a rapid rate. Attempts have been made to produce mutant of PON-1 that are more catalytically efficient and potentially protective against nerve agents (Masson, 2011).

1.3.2 Anticholinergics

Atropine is a muscarinic acetylcholine receptor antagonist that helps to decrease the effects of ACh in muscarinic synapses (Masson, 2011). It accomplishes this by blocking the binding of ACh to muscarinic receptors in smooth and cardiac muscle, glands, peripheral ganglia, and the CNS. Both atropine and AChE compete for a common binding site on these receptors. Due to its competitive nature, this inhibition can be overcome with sufficient ACh concentrations. Atropine counteracts many of the ill effects of OPs including bronchoconstriction, heart block and excess glandular secretions. Its effects begin within 1-4 minutes of administration and peak within 8 minutes (Brown & Taylor, 2006; Gallo & Lawryk, 1991).

1.3.3 Oximes

Oximes are a group of compounds that can be used to reactivate phosphorylated AChE. This ability comes from their oximate anion, which is strongly nucleophilic at a physiological pH (Masson, 2011). Nucleophilic attack by oximes releases the bound OP moieties from AChE (Gallo & Lawryk, 1991). There is no recognized best oxime as their reactivation potential differs depending on which OP has phosphorylated AChE. Once an AChE bound OP has aged oximes no longer have the ability to remove the group.

Currently used oximes such as 2-PAM, obidoxime, and HI-6 are quaternary pyridinium oximes. These oximes are able to reactivate peripheral AChE restoring respiratory function and decreasing mortality. They are strongly charged and thus unable

to cross the BBB. This prevents them from attenuating CNS damage caused by OP intoxication. Various attempts have been made to facilitate delivery to the brain, but none have been successful enough for field use (Masson, 2011).

1.3.4 Intoxication Treatment

In cases of organophosphate exposure, treatment differs somewhat depending upon the level of intoxication. In less severe cases of OP intoxication, atropine sulfate is administered first. Once atropine has been administered, decontamination of any remaining source of OP will prevent further entry of the chemical into the body. Should the victim fail to respond to atropine alone, pralidoxime chloride (2-PAM) would be administered. Beyond that, treatment is symptomatic. In more severe cases, artificial respiration is the most immediate priority. Next, multiple higher doses of atropine than used in less severe exposures are administered followed by 2-PAM therapy. After medications have been administered, decontamination and symptomatic treatment can be performed (Gallo & Lawryk, 1991).

1.4 Novel Oximes

While conventional pyridinium oximes such as 2-PAM are effective at decreasing mortality in those exposed to high OP doses, they have little to no ability to cross the blood brain barrier and reactivate AChE within the central nervous system. It is believed that an oxime that could effectively cross the BBB and reactivate AChE within the CNS could both increase chances of survival and prevent or attenuate seizures and resultant brain injury in those exposed to these compounds, reducing the burden of neurological disease in these individuals.

A series of novel pyridinium oximes (US patent 9,277,937) with the potential to penetrate the blood brain barrier has been invented by Dr. Howard Chambers in the Department of Biochemistry, Molecular Biology, Entomology and Plant Pathology at Mississippi State University. These novel oximes have shown promising results in reactivating brain AChE in both *in vitro* and *in vivo* rat studies. This testing has been conducted using two highly relevant surrogates of sarin and VX, nitrophenyl isopropyl methyl phosphonate (NIMP) and nitrophenyl ethyl methyl phosphonate (NEMP), respectively (Meek et al., 2012). Oximes were administered at the time of peak brain AChE inhibition in order to ensure that decreased inhibition of brain AChE was the result of oxime entry into the brain and not due to the OP being bound by reactivated peripheral AChE, decreasing the amount of OP able to reach the brain. In the *in vitro* studies, some oximes have achieved AChE reactivations of 70%. *In vivo* studies were subsequently conducted on oximes that reached a minimum of 40% *in vitro* reactivation. The most successful of these oximes, Oxime 20, achieved AChE reactivation of 25% in brain tissue at 30 min post oxime administration. In this same *in vivo* study, 2-PAM produced no AChE reactivation within the brain. While degree of lipophilicity was not related to efficacy at reactivating AChE, all of the tested oximes were more lipophilic than 2-PAM, possibly explaining their ability to reactivate brain AChE (Chambers, Chambers, Meek, & Pringle, 2013). Further studies produced *in vivo* brain AChE reactivation of up to 35% at 2 hours post oxime administration. Oxime 20 (the most effective reactivator of AChE within the brain thus far) has levels of peripheral AChE reactivation approaching that of 2-PAM, 40 to 45% compared to 55 to 60%. Studies of seizure attenuation and survival using lethal doses of NIMP and NEMP demonstrated the protective effect of both Oxime

20 and Oxime 1. Both of these oximes caused termination of seizures by 6 hours while rats treated with 2-PAM were still displaying seizure activity at 8 hours. Additionally, the novel oximes produced higher survival rates than 2-PAM (Chambers et al., 2016).

Studies have also been performed of astrocyte glial fibrillary acidic protein (GFAP) expression in rat brains following exposure to nerve agent surrogates as an indicator of activation of astrocytes, which should indicate neuroinflammation. Seizure behavior and increased GFAP expression of both NIMP and NEMP treated rats were similar to those of the positive control, kainic acid. GFAP levels in those rats subsequently treated with Oxime 20 showed lower levels of GFAP relative to OP alone, similar to the control, indicating that brain inflammation would likely be greatly reduced or eliminated in subjects receiving this therapy. In contrast to Oxime 20, 2-PAM was not observed to affect level of GFAP expression in this study.

1.5 Research Summary

To further study the potential use of these novel oximes, the research described in this thesis was undertaken. This work sought to further measure the sparing of neuronal injury resultant of OP intoxication when these oximes were employed. The first goal of this research, as will be discussed in Chapter 2, was to compare degree of neurodegeneration seen in the brains of rats dosed with the sarin surrogate NIMP or paraoxon to those of rats that were dosed with NIMP but subsequently treated with one of our lead novel oximes, Oxime 20. The next goal was to further explore how the cells of the CNS respond physiologically to NIMP administration and treatment of NIMP intoxication with Oxime 20, Oxime 1, and 2-PAM. Genetic regulation of MAP kinase was selected for this as this system mediates cellular response to a variety of stimuli and

may provide insight into how these cells will respond to exposure to these compounds. This experiment will make up Chapter 3 of this document.

CHAPTER II

NEURODEGENERATION FOLLOWING ORGANOPHOSPHATE AND NOVEL OXIME TREATMENT

2.1 Introduction

Organophosphates, especially those used as pesticides or CWAs, function as potent cholinesterase inhibitors capable of producing various toxic signs including hypersecretion, convulsions, coma, and death. Depending on dose and agent of exposure, seizures can progress rapidly into full status epilepticus that can produce significant brain damage. Work in rats using soman shows that acetylcholinesterase inhibition leads to a build-up of acetylcholine, which causes excessive cholinergic stimulation resulting in seizures, the first 5 minutes of which are completely dependent on cholinergic stimulation. During the time from 5 minutes to 40 minutes after induction of seizures, control of seizure activity begins to transition from the cholinergic system to other neurotransmitters (Shih & McDonough, 1997). Once seizures begin, extracellular glutamate levels increase and serve as the main source of seizure stimulation (Lallement et al, 1991). Past 40 minutes of seizures, the cholinergic system no longer serves as the primary controller of seizure activity, and excitatory amino acids such as glutamate are the main source of seizures (Shih & McDonough, 1997; Eisenkraft, Falk, & Finkelstein, 2013). As a result of these prolonged seizures, excitotoxic neural pathology occurs following exposure to high dosages of organophosphate anticholinesterases (McDonough, Dochterman, Smith, & Shih, 1995). Status epilepticus resulting from OP

exposure has been documented to produce a prolonged elevation of calcium within the brain that could be indicated in the excitotoxic neuropathology due to the important role that calcium ions play as second messengers in neurodegenerative pathways (Deshpande, Carter, Blair, & DeLorenzo, 2010; Deshpande, Blair, Phillips, & DeLorenzo, 2016b). This damage results in some cells dying within the first 24 hours. During this same time course, some neurons develop an eosinophilic, degenerate appearance. These neurons will degenerate and die in a period of time ranging from 2 weeks to 2 months (Collombet et al., 2011). On closer examination, these degenerating neurons display necrotic, apoptotic, and hybrid forms of cell death. One study of ultrastructural morphology demonstrated at least 11 distinct morphological types of degrading neurons displaying varying degrees of both apoptotic and necrotic characteristics as a result of soman exposure (Baille et al, 2005). The death of these degenerating neurons can provide a source of further damage lasting out to three months post-OP exposure. Beyond 3 months, there should be no further degenerate neurons present (Collombet et al., 2011).

Studies of organophosphate induced neurodegeneration show widespread, highly variable neuronal damage in the brains of exposed animals. Of the damage seen with these compounds, six regions most consistently displayed neurodegeneration. These regions are the piriform cortex, hippocampus, thalamus, amygdala, cerebral cortex, and caudate/putamen. The piriform cortex, amygdala, and hippocampus tend to most frequently display evidence of neuropathology, while the piriform cortex and hippocampus are generally the most severely damaged of these regions. Within these regions of the brain, certain subsets of cells seem to be more sensitive to the effects of OPs. In the piriform cortex, the pyramidal cells are primarily affected. The CA1 and CA2

regions of the hippocampus suffer more damage than the CA3. The medial and dorsal nuclei of the thalamus generally suffer more damage than other areas within this region. Damage in the cerebral cortex is usually less than other areas of the brain with occasional necrosis of pyramidal cells. Damage to the caudate/putamen is generally both less frequent and less severe than other areas of the brain (McDonough, Jaax, Crowley, May, & Modrow, 1989; McDonough et al., 1995). The specificity of this excitotoxic damage in these regions could be explained by the dense association of cholinergic neurons and the large number of cholinergic projections (Chen, 2012).

Aside from direct damage to the neurons resulting from seizures, the subsequent metabolic deregulation and cell death result in activation of microglia and astrocytes producing neuroinflammation (Collombet et al., 2011). Glutamate itself can contribute to this activation of the immune system. Evidence exists that T cells can be activated directly by glutamate and subsequently activate microglia by the secretion of cytokines (Eisenkraft et al., 2013). These activated microglia and astrocytes along with invading macrophages produce inflammatory cytokines for several days following neuronal injury. These inflammatory cytokines, of which microglia are the primary source, include tumor necrosis factor α (TNFα), interleukin 1β (IL1β) and interleukin 6 (IL6). Astrocytes additionally produce neurotrophic factors and growth factors including ciliary neurotrophic factor (CNTF), brain-derived neurotrophic factor (BDNF), basic fibroblast growth factor (FGF-2), nerve growth factor (NGF) and vascular endothelial growth factor (VEGF). These cytokines contribute to the survival of degenerating neurons and also promote glial scar formation (Collombet et al., 2011).

Astrocytes are glial cells that serve several important functions following brain injury. Several of these functions, including taking up excess extracellular glutamate and eliminating reactive oxygen species, protect neurons after an acute injury. They can also serve a role in the inflammatory processes that occur following an injury by secreting an array of inflammatory cytokines. Following injury and destruction of neurons, astrocytes can form glial scars within the brain as well as assist in remodeling of the extracellular matrix. Astrocytes also produce neurotrophic factors that assist in survival and remodeling of neurons following injury (Chen & Swanson, 2003). In rodents, astrocytes are typically activated within 3 days post-traumatic brain injury, and this activation can last for several weeks (Collombet et al., 2007).

Microglia are activated in a timespan from hours to days following a neurodegenerative event to serve as the main inflammatory cell within the brain. Once activated, their morphology and antigen expression begin to become more macrophage-like, and they exhibit some functions similar to macrophages such as phagocytosis of cellular debris and secretion of inflammatory cytokines (Zimmer, Ennis, & Shipley, 1997; Simoni et al., 2000).

The damage produced in the brain as a result of OP intoxication can lead to long-lasting behavioral and cognitive impairment (Filliat et al., 2006). Current treatment for OP intoxication in the United States involves the use of atropine, anticonvulsants, and the oxime 2-PAM. Atropine has anticholinergic effects, antagonizing excess ACh at muscarinic receptors. Anticonvulsants such as diazepam are capable of terminating seizures by acting on GABA receptors. Oximes act by transphosphorylating OP molecules that are bound to AChE. This reactivates the AChE molecule and makes it

available to degrade ACh. The currently approved oxime for the treatment of OP intoxication in the U.S. is pralidoxime (2-PAM) (RamaRao, Afley, Acharya, & Bhattacharya, 2014). While 2-PAM is effective at decreasing mortality in those exposed to high OP doses, it has little to no ability to cross the blood brain barrier and reactivate AChE within the CNS. It is believed that an oxime that could effectively cross the BBB and reactivate AChE within the CNS could both increase chances of survival and prevent or attenuate seizures and resultant brain injury in those exposed to these compounds, reducing the burden of neurological disease in these individuals.

A series of novel phenoxyalkyl pyridinium oximes developed by Dr. Howard Chambers at the Department of Biochemistry, Molecular Biology, Entomology and Plant Pathology at Mississippi State University have been shown to have the potential to be more effective than oximes currently available in both preventing mortality and decreasing morbidity (in the form of brain damage) in rats exposed to high doses of OPs. The novel oximes have shown promising results of reactivating brain AChE in both in vitro and in vivo studies. This testing has been conducted using two highly relevant surrogates of sarin and VX, nitrophenyl isopropyl methyl phosphonate (NIMP), first described by Ohta et al. (2006), and nitrophenyl ethyl methyl phosphonate (NEMP), first described by Fukuto & Metcalf (1958), respectively (Meek et al., 2012). Oximes were administered at the time of peak brain AChE inhibition following a high sublethal dose of organophosphate. This time was chosen to ensure that decreased inhibition of brain AChE was the result of oxime entry into the brain and not due to the OP being bound by reactivated peripheral AChE, decreasing the amount of OP able to reach the brain. In the in vitro studies, some oximes have achieved AChE reactivations of 70%. In vivo studies

were subsequently conducted on oximes that reached a minimum of 40% in vitro reactivation. The most successful of these oximes, Oxime 20, achieved AChE reactivation of 25% in brain tissue at 30 minutes post oxime administration. In this same in vivo study, 2-PAM produced no AChE reactivation within the brain. While degree of lipophilicity was not related to efficacy at reactivating AChE, all of the tested oximes were more lipophilic than 2-PAM, possibly explaining their ability to reactivate brain AChE (Chambers et al., 2013). Further studies produced in vivo brain AChE reactivation of up to 35% at 2 hours post oxime administration. Those oximes that reactivated at least 20% of brain AChE attenuated seizures. Oxime 20 (the most effective reactivator of AChE within the brain thus far) has levels of peripheral AChE reactivation approaching that of 2-PAM, 40 to 45% compared to 55 to 60%. Treatment with these compounds has been shown to produce survival rates comparable to or better than 2-PAM and attenuate seizure like-behavior (Chambers et al., 2016).

Previous studies have been performed measuring GFAP expression in rat brains following exposure to nerve agent surrogates and subsequent treatment with Oxime 20 as an indicator of neurodegeneration. It was observed that GFAP expression in the piriform cortex and dentate gyrus was significantly reduced in animals treated with Oxime 20 at 4 days post-exposure to NIMP or NEMP challenge relative to those that were not treated with the novel oxime. Seizure behavior and GFAP expression of both NIMP and NEMP treated rats were similar to those of the positive control, kainic acid. GFAP levels in those rats subsequently treated with Oxime 20 showed decreased levels of GFAP, similar to the control, indicating that brain damage would likely be greatly reduced in subjects

receiving this therapy. In contrast to Oxime 20, 2-PAM was not observed to affect the level of GFAP expression in that study.

This study was designed to further examine neural damage induced by the sarin surrogate NIMP and paraoxon and explore the ability of the novel oximes to attenuate this damage. Development of observable pathological signs is attributed to prolonged seizure activity. Compounds that are able to prevent or attenuate seizures have been shown to decrease resulting pathology (McDonough et al., 1995). For this study, lethal doses of both NIMP and paraoxon were used in order to produce excitotoxic neurodegeneration. Time delays of 1 hour between OP and oxime administration were included to reflect the delay that would occur in actual poisoning events. As the brain can tolerate about 45 min of seizures without appreciable neurodegeneration (Motte, Fernandes, Baram, & Nehlig, 1998; Norwood et al., 2011), a 1 hour delay, reflecting the observed 15 minute latent period and 45 minutes of seizures, is an approximate far end of the therapeutic window needed for preventing brain damage. The test dosage of novel oximes was 146 μmoles/kg, the molar equivalent of the approved therapeutic dosage of 2-PAM delivered in three auto-injectors. This dosage has been chosen because it would best emulate treatment of human poisoning victims. The novel oximes chosen for this study were Oxime 20 and Oxime 15, two of the most promising of the novel oximes. Neurodegeneration was measured at both 24 hours and 4 days post-organophosphate exposure. Twenty-four hours was chosen as to measure immediate excitotoxic neurodegeneration while four days was selected to examine delayed neurodegeneration. In the 24 hour brains, the hippocampus, amygdala, and piriform cortex were selected for examination due to their high incidence and severity of neurodegeneration as noted in

published literature. For 4 day animals, these regions were limited to the hippocampus and piriform cortex due to their higher incidence of damage noted in published literature.

For measurement of neurodegeneration, FluoroJade B provides an easily quantifiable, highly specific measure of dying neurons (Schmued, Albertson, & Slikker, 1997; Schmued & Hopkins, 2000). The use of this stain has been previously described in animal model studies of nerve agent exposure (Myhrer, Andersen, Nguyen, & Aas, 2005; Myhrer, Enger, & Aas, 2006; Apland et al., 2010; RamaRao et al., 2014; Li et al., 2011). As this stain is not selective for either necrotic or apoptotic processes, it provides a measure of total dying neurons, which are seen to display varying degrees of necrotic and apoptotic properties (Baille et al., 2005). Additionally, as not all neurons that will die from OP intoxication die immediately, staining these degenerating cells gives a measure of the degree of neuronal death that is expected to occur but has not yet been completed. To assist in identifying locations within the brain, DAPI was used as a counterstain to indicate intact neurons (Giorgi et al., 2003). For verification of this staining method, kainic acid was used as a positive control for neurodegeneration (Schmued & Hopkins, 2000).

2.2 Methods

2.2.1 Kainic Acid Treatments

Adult male (250-300g) Sprague Dawley rats were injected intraperitoneally with 10mg/kg kainic acid dissolved in sterile water. Initially, kainic acid sourced from Cayman Chemical Companey (Ann Arbor, MI) was used for these treatments. Due to lack of solubility and efficacy in producing seizures, kainic acid was purchased from Tocris Bioscience (Bristol, UK), which proved highly soluble and effective in producing

seizures. Rats were monitored for 8 hours following initial injection and maintained by animal facility staff for the next 24 hours to 4 days.

2.2.2 Organophosphate Treatments

Adult male (250-300g) Sprague Dawley rats were injected subcutaneously with either a lethal dosage of the sarin surrogate NIMP (0.6 mg/kg), a lethal dosage of paraoxon (0.8 mg/kg), or vehicle (Multisol). Oximes were given 30 minutes after organophosphate administration. An intramuscular injection of 146 μmol/kg of either Oxime 20, Oxime 15, or 2-PAM or vehicle (Multisol) was administered to rats in those treatment groups. The first dose of atropine was also administered intramuscularly at a dosage of 0.65 mg/kg at this time. Over the first 4 hours rats were administered up to 2 additional injections of atropine as necessary for control of peripheral cholinergic signs with most rats receiving 3 injections total. Rats were monitored for 8 hours following initial injection and maintained by animal facility staff for the next 24 hours to 4 days. These procedures were performed under an approved Institutional Animal Care and Use Committee protocol (#17248).

2.2.3 Perfusion and Sample Processing

Twenty-four hours or four days after treatment, rats were perfused by a protocol adapted from (Gage, Kipke, & Shain, 2012). The rats were deeply anesthetized with isoflurane and transcardially perfused with 0.9% sodium chloride until fluid ran clear followed by 200 ml 4% paraformaldehyde. Skulls were removed and stored in paraformaldehyde for 24 hours. At that point the brains were removed and placed in 25% sucrose for 4 days to allow equilibration of sucrose into the brains to protect the architecture of the tissue during freezing. At 4 days the brains were flash frozen in

isopentane chilled over dry ice and then stored at -80^0 C until sectioning. The brains were sectioned on a Leica HM560 cryostat with 25 μm sections taken 200 μm apart beginning approximately 1.5 mm anterior to the bregma and ending 5mm posterior of the bregma. These sections were mounted onto gelatin-coated slides and dried overnight at room temperature.

2.2.4 Fluoro-Jade B Staining

The prepared slides were rehydrated in distilled water for 5 minutes prior to staining. The slides were immersed in 0.06% potassium permanganate for 20 minutes on an orbital shaker. This step serves to decrease background staining and decrease fading of the stain from either age or exposure to light (Schmued et al., 1997). Slides were rinsed three times for one minute each in dH2O. Slides were next placed in Fluoro-Jade B/DAPI working solution in a light protected vessel on the orbital shaker for 30 minutes. This working solution was created by adding to 165 ml 0.1% acetic acid: 7 ml Fluoro-Jade B (Histo-Chem Inc., Jefferson AR) 0.01% stock solution and 3 ml DAPI (Thermo Scientific, Rockford Il) 0.01% stock solution for a total working volume of 175 ml (Schmued & Hopkins, 2000). Slides were again rinsed 3 times for 1 minute each in dH2O. Sections were dehydrated by a graded alcohol series of 70%, 90%, and 100% ethanol with 3 minutes in each alcohol followed by 5 minutes in xylene to clear sections for mounting. DPX mounting media was used to coverslip the slides. Slides were then air-dried in the dark and stored in a slide box until imaging.

2.2.5 Data Quantification

An Olympus U-MWB blue 450-480 nm excitation filter was used to induce Fluoro-Jade B light emission. Slides were examined and images taken on an Olympus

BX60 microscope at the 40X objective with a Lumenera Infinity 3 microscopy camera. All samples were measured with the counter blinded to their treatment.

Twenty-four hour brains were examined first. In these samples, all regions of each section were fully counted for Fluoro-Jade B staining. Any slide with greater than 100 counts was considered "too numerous to count" (TNTC). Following this study, it was determined that this method was too thorough for those brains displaying significant neurodegeneration while not providing any experimental benefit for those that were not, so a different method was selected for 4 day animals.

For 4 day samples, three images were taken of high-power fields of the hilus of the hippocampus, the CA1 region of the hippocampus, and the piriform cortex. This was performed for each brain within sections that approximate -2.8 mm, -3.6 and -4.16mm posterior to the bregma according to *The Rat Brain in Stereotaxic Coordinates: Hard Cover Edition* (Paxinos & Watson, 2006). Fluoro-Jade B positive staining cells were counted in each of these images and compiled into an Excel spreadsheet for data analysis. ImageJ was used to assist in counting images containing high numbers of Fluoro-Jade B positive cells (Schneider, Rasband, & Eliceiri, 2012). Counts were compiled into Excel for analysis.

2.3 Results

Rats treated with kainic acid from Cayman produced signs of intoxication ranging from mild depression to facial tremors. These rats showed no neurodegeneration upon tissue processing. Rats treated with kainic acid from Tocris showed signs of seizure activity including rearing and falling with forelimb clonus and death. The animals

receiving this treatment displayed significant neurodegeneration upon tissue processing verifying that the Fluoro-Jade B stain properly labeled degenerate neurons and that this staining was present both at 24 hours and 4 days.

In total 115 rats were dosed per the organophosphate treatment protocol described with perfusion and tissue preparation proceeding accordingly. Thirty-two of these animals were perfused at a 24 hour time point, and 83 were perfused at a 4 day time point.

In the 24 hour perfusion group, 4 brains were considered TNTC leaving 28 that were fully counted. Due to differences in how many brains were available in each treatment group and how many sections each brain produced, cells counted were expressed both as total counts and counts per section (Table 2.1). Counts per section ranged from 0.19 positive cells per section in the piriform cortex of the Paraoxon + Oxime 20 group to 2.16 cells per section in the hippocampus of the Vehicle control. Due to the very low number of counts in these brains and the fact that the vehicle control counts were not appreciably different from any of the other treatments, the counts in these groups are likely due to a basal stain uptake or a standard production of artifacts from the staining methods employed.

The brains that were considered TNTC showed the distinct architecture of degenerating neurons confirming that the Fluoro-Jade B staining was that of degenerating neurons. The number of positive cells in each section from these brains far exceeded the minimum 100 counts to be considered TNTC. Of the 4 brains counted as TNTC, 3 were treated with Paraoxon 0.8 alone and 1 was treated with both Paraoxon 0.8 and Oxime 20. There was a noticeable day effect in this as two of the Paraoxon 0.8 and the Paraoxon 0.8

+ Oxime 20 were from two consecutive treatment days. No Paraoxon + 2-PAM rat survived to perfusion from either of these days for comparison. No rat dosed with NIMP and perfused at 24 hours displayed neurodegeneration.

Following this study, it was determined that measurement parameters should be focused on examining those brains that exhibited significant neurodegeneration. For the rats perfused at 4 days, images were taken from several high-power fields of the hilus and CA1 regions of the hippocampus and the piriform cortex for Fluoro-Jade B quantification. Of the animals perfused at 4 days, the only rats that displayed significant neurodegeneration were within NIMP 0.6, paraoxon (Pxn) 0.8, and Pxn 0.8 + 2-PAM treatment groups. Numbers of animals that displayed neurodegeneration out of these groups were: 2 of 15 NIMP 0.6 rats, 2 of 13 Pxn 0.8 rats, and 2 of 12 Pxn 0.8 + 2-PAM rats. No rat treated with the novel oximes displayed neurodegeneration at 4 days nor did vehicle control animals or NIMP 0.6 + 2-PAM treated animals. The general analysis of these animals is described in Table 2.2.

The distribution and severity of neurodegeneration in those animals displaying positive Fluoro-Jade B staining appeared to be highly variable. Table 2.3 details the counts by region and section of the animals that showed Fluoro-Jade B staining. It can be observed in these counts that there is not one section or region of the brain that consistently shows damage more than any other. Even between animals administered the same treatment, distribution and severity of degenerating neurons was not consistent. Possibly the best example of this is between the two NIMP treated animals. The first of these treated on February 23 showed much more damage in the CA1 region of the -3.6

and -4.16 sections while the other showed much less damage in this region, hardly any in the hilus, and much more in the piriform cortex than the other animal.

Table 2.4 summarizes the counts from these animals into averages based on treatment group. While this average decreases the variability of the observed counts to a degree, the organophosphates still produced a variable distribution of Fluoro-Jade B positive cells.

2.4 Discussion

Kainic acid treatment of rats verified that Fluoro-Jade B positively stains degenerating neurons with the procedure described here. This staining was visible both at 24 hours and at 4 days post-treatment. Additionally, positive Fluoro-Jade B staining of rats treated with organophosphates was of similar appearance to those treated with kainic acid.

The results of the animals perfused 24 hours post-OP treatment demonstrate that administration of paraoxon was capable of producing appreciable neurodegeneration. While no neurodegeneration was seen with the treatment of paraoxon with 2-PAM, only one sample was available for this group and serves as a poor indicator for the outcome of this treatment. One animal that was treated with paraoxon and Oxime 20 displayed significant neurodegeneration. This indicates that Oxime 20 is not fully neuroprotective in all animals, but the incidence of this damage was much lower than with paraoxon alone. It should be noted that a day effect might have played a role in this outcome as the one Oxime 20 treated brain with neurodegeneration came from one of two consecutive days in which all surviving rats, except one other that also received Oxime 20, stained positive with Fluoro-Jade B. No rat treated with paraoxon and 2-PAM on these days

survived to perfusion for comparison. It is likely that variability in either the concentration of the paraoxon preparation or the susceptibility of that group of rats to organophosphates led to this outcome. Contrary to the paraoxon data for this time point, the lethal dose of NIMP did not produce appreciable neurodegeneration in any of the observed samples. This is despite the animals' seizure-like behavior appearing similar between OPs and NIMP producing neurodegeneration at the 4 day time point at a similar rate as paraoxon. It has been speculated that due to the pharmacokinetics of this compound differing from paraoxon and sarin, neurodegeneration could be a more delayed event in these animals. Alternatively, due to the smaller number of animals used in this study, there may have not been enough power to observe the rate of neurodegeneration produced by NIMP at a 24 hour time point. In total, 50% of animals dosed with paraoxon alone displayed appreciable neurodegeneration while only 17% showed neurodegeneration when Oxime 20 treatment was employed. No other treatment groups displayed significant neurodegeneration.

The results of the 4 day time point effectively demonstrated that lethal doses of both NIMP and paraoxon are capable of producing neurodegeneration in the rat model of organophosphate exposure. Following NIMP exposure, 13% of rats displayed significant neurodegeneration while with paraoxon treatment 15% of rats demonstrated significant damage. Rats dosed with paraoxon and treated with 2-PAM displayed neurodegeneration at a rate of 17% of rats. No rat administered NIMP with 2-PAM showed any sign of neurodegeneration. None of the rats that were dosed with either NIMP or paraoxon and then treated with Oxime 20 or Oxime 15 displayed any significant neurodegeneration (Table 2.2). This is suggestive that the novel oximes afford protection against

neurodegeneration. By controlling OP induced seizure activity from acetylcholine accumulation, these compounds should prevent neuropathology from persistent seizures (McDonough et al., 1995; Baille et al., 2005; Chapman, Kadar, & Gilat, 2007; Shih, Duniho, & McDonough, 2003).

As NIMP is not a widely used surrogate of sarin exposure, these results cannot be compared to existing literature for this compound. It can be remarked that similar to research with other organophosphates, the neurodegeneration produced by NIMP is variably distributed throughout several structures within the brain. Unlike this previous work, which used male Sprague Dawley rats treated with sarin at 180 μg/kg subcutaneously producing neurodegeneration in 98% of animals treated, the treatment of NIMP 0.6 mg/kg subcutaneously in this study produced no neurodegeneration at the 24 hour time point and neurodegeneration in only 13% of NIMP alone treated animals at the 4 day time point (McDonough et al., 1995).

Paraoxon has been used in other published research and has been shown to produce neurodegeneration with dosages ranging from 0.45 mg/kg to 4 mg/kg (Finkelstein et al., 2012; Deshpande, Blair, Huang, Phillips, & DeLorenzo, 2016a; Krishnan et al., 2016). Deshpande, Carter, Phillips, Blair, and DeLorenzo (2014b) examined a range of doses of paraoxon alone in male Sprague Dawley rats ranging from 0.1 mg/kg to 8 mg/kg. At a dose of 0.8 mg/kg they observed 71% of treated animals undergoing status epilepticus with a mortality rate of 50%. Doses of 2 and 4 mg/kg of paraoxon alone produced status epilepticus at rates of 90% and 100% respectively both with 100% mortality. In exploring a model of neurodegeneration, this study used a dose of 4 mg/kg paraoxon. A lower dose of atropine similar to auto-injector doses decreased

mortality by 20%, but in the interest of producing a survival model, the investigators explored a higher dose. This dose was increased to 2 mg/kg, which when given with 25 mg/kg 2-PAM resulted in a survival rate of 50% at 24 hours. Racine scores of animals in this study were not affected either by atropine or 2-PAM, alone or in combination. The dosage of paraoxon used in the study described here is on the low end of doses from published literature but higher incidences of neuropathology have been seen with lower doses than used in this study. It could be that unknown variables make the animals in the model used in this study more resistant to neurodegeneration necessitating the use of a dose on the higher end of published literature. Published studies indicate that sensitivity of rats to kainic acid, a model inducer of seizures and excitotoxic neurodegeneration, can differ between strains of animal, so this possibility is not without basis (Golden, Smith, Ferraro, & Reyes, 1995).

At the 4 day time point, lethal doses both of NIMP and paraoxon alone produced neurodegeneration in a small percent of animals while no animal treated with Oxime 20 or Oxime 15 displayed evidence of neurodegeneration. Previous studies of anticonvulsant therapy of the nerve agent soman using benzodiazepines or centrally active anticholinergics provided evidence that control of seizure activity decreased both incidence and severity of neuropathology in their animal model giving validity to the assertion that attenuation of seizure activity by the novel oximes could contribute to the lack of neurodegeneration (McDonough et al., 2000).

Comparing 24 hour and 4 day perfusion time points, NIMP only produced neurodegeneration at the 4 day time point. As previously discussed, this could be due to a delayed onset of NIMP induced neuropathology or a matter of study power at the 24

hours time point. Paraoxon alone displayed neurodegeneration in 50% of animals at 24 hours and 15% at 4 days. A recent study with the sarin surrogate DFP demonstrated that neuronal necrosis is visible as early as 12 hours after DFP exposure and persisted up to 60 days post-exposure (Siso et al., 2017). Both of the time points from the current study fall into the range at which these changes would be present.

There were no clear differences observed in the quantity or distribution of Fluoro-Jade B positive neurons between treatments that produced observable neurodegeneration at the 4 day time point. This likely indicates that the anticholinergic activity and resulting excitotoxicity display similar activities in both NIMP and paraoxon treated animals.

2.5 Conclusion

The examination of excitotoxic neurodegeneration is an important aspect of the investigation of both the organophosphate exposure models used here and the novel pyridinium oximes intended for the treatment of organophosphate intoxication. Neurodegeneration is a well-documented outcome of CWA exposure, and neuronal damage has been linked to behavioral alterations and cognitive impairment (Deshpande, Phillips, Huang, & DeLorenzo 2014a; Myhrer et al. 2005). By examining neurodegeneration in rats treated with NIMP and paraoxon, it is possible to compare this model of nerve agent exposure to models using nerve agents and other nerve agent surrogates in terms of neuronal damage. The ability of the novel oximes to attenuate neurodegeneration serves as an important indicator of the protective potential of these treatments. Control of OP induced seizures is critical in the prevention of neuropathology, as persistent seizure activity from the accumulation of acetylcholine and

glutamate is strongly associated with brain damage (McDonough et al., 1995; Baille et al., 2005).

The data in this study support that NIMP and paraoxon have the potential to serve as highly relevant surrogates of OP CWA induced neuropathology. In animals that displayed significant Fluoro-Jade B staining, the distribution and severity of lesions roughly approximated the findings of previous research using live nerve agents. Compared to published literature, the percent of animals that showed neurodegeneration from seizure activity was relatively low in this study. The small percent of brains in which neurodegeneration was seen poses a practical problem in the large number of animals that would likely be needed for statistical power, both in terms of necessary labor and quantities of research materials. As such it might be practical to perform range-finding studies to examine incidence and severity of neurodegenerative lesions with various doses of NIMP and paraoxon. As indicated by previous research, higher doses of atropine and standard use of the oxime 2-PAM in those animals not receiving the novel oximes may be necessary for an acceptable survival rate in those animals receiving higher OP doses while not hindering the production of neural pathology.

These initial findings of the use of Oxime 20 and Oxime 15 to prevent OP induced neurodegeneration are promising. At the 24 hour time point, Oxime 20 greatly reduced the percent of paraoxon animals that showed Fluoro-Jade B staining. At the 4 day time point, no animal given the novel oximes stained positive for neurodegeneration while several that did not receive the novel oximes demonstrated measurable neurodegeneration.

Table 2.1 Summary of Fluoro-Jade B Staining 24 Hours Post-OP Exposure

			NIMP 0.6	NIMP 0.6 + OX20	NIMP 0.6 + 2PAM	PXN 0.8	PXN 0.8 + OX20	PXN 0.8 + 2PAM	Vehicle
Total Brains	**Number of brains**	**n=**	5	5	2	6	6	1	7
Countable Brains	**Total Counts[1]**	**HC**	100	98	30	150	49	16	238
		PC	49	37	16	29	27	8	35
		AM	37	29	8	85	15	10	144
	Counts/Section[2]	**HC**	1.35	1.37	1.20	3.22	0.70	1.07	2.16
		PC	0.36	0.24	0.33	0.98	0.19	0.26	0.59
		AM	0.53	0.43	0.32	2.73	0.22	0.67	1.85
TNTC Brains	**TNTC[3]**		0	0	0	3	1	0	0
	% TNTC[4]		0%	0%	0%	50%	17%	0%	0%

Summary of Fluoro-Jade B data of brains of all rats dosed with either nitrophenyl isopropyl methyl phosphonate (NIMP) 0.6 mg/kg or paraoxon (PXN) 0.8 mg/kg subcutaneously with some receiving Oxime 20 (OX20) or pralidoxime (2PAM). Rats were perfused at the 24 hour time point and brains were stained with Fluoro-Jade B. Data are grouped by treatment. The data are expressed both as the total of all counts from all of the counted sections from each brain from each treatment group[1] and the average counts by the number of sections counted to adjust varying number of sections between treatments and regions[2]. Regions selected for these counts were the hippocampus (HC), piriform cortex (PC), and amygdala (AM). Also represented are brains that were considered TNTC (greater than 100 positive cells per region) both as a total of how many brains were TNTC[3] and what percent of brains within a treatment group were TNTC[4].

Table 2.2 Summary of Fluoro-Jade B Staining 4 Days Post-OP Exposure

		NI 0.6	NI 0.6 + 2PAM	NI 0.6 + OX20	NI 0.6 + OX15	PXN 0.8	PXN 0.8 +2PAM	PXN 0.8 + OX20	PXN 0.8 + OX15	MULTISOL
TOTAL[1]	CA1	340	1	1	1	70	49	2	0	1
	HILUS	199	1	0	1	261	208	3	0	1
	PC	599	2	3	0	976	354	2	2	2
AVERAGE[2]	CA1	23	0	0	0	5	4	0	0	0
	HILUS	13	0	0	0	20	17	0	0	0
	PC	40	0	1	0	75	30	0	0	0
Standard Deviation[3]	CA1	81	0	0	0	13	9	0	0	0
	HILUS	34	0	0	0	49	41	1	0	0
	PC	107	1	1	0	198	81	0	1	0
Total Brains[4]		15	6	6	7	13	12	7	6	11
Damaged Brains Total[5]		2	0	0	0	2	2	0	0	0
Percent Damaged[6]		13%	0%	0%	0%	15%	17%	0%	0%	0%

Summary of Fluoro-Jade B data of brains of all rats dosed with either nitrophenyl isopropyl methyl phosphonate (NIMP) 0.6 mg/kg or paraoxon (PXN) 0.8 mg/kg subcutaneously with some receiving Oxime 20 (OX20), Oxime 15 (OX15), or pralidoxime (2PAM). Rats were perfused at the 4 day time point and brains were stained with Fluoro-Jade B. Data are grouped by treatment. Includes counts expressed both as the total[1] and average[2] counts per brain by region as well as the standard deviation[3]. Also included are total number of brains in each treatment group[4], number of brains that showed appreciable damage[5], and this number expressed as a percentage[6]. Regions selected for these counts were the CA1 and hilus of the hippocampus and the piriform cortex (PC).

Table 2.3 4 Day Fluoro-Jade B Positive Brains – by Individual

Section[1]	Region[2]	2/23/17	4/13/17	3/20/17	6/8/17	3/20/17	3/20/17
		NIMP .6	NIMP .6	PXN .8	PXN .8	PXN .8 +2PAM	PXN .8 +2PAM
-2.8	CA1	17	4	21	23	19	4
	HILUS	51	1	62	106	53	31
	PC	29	117	70	157	70	15
-3.6	CA1	85	10	8	14	9	5
	HILUS	25	1	42	85	37	35
	PC	33	114	95	151	84	31
-4.12	CA1	211	21	3	24	3	5
	HILUS	25	0	36	98	35	17
	PC	38	95	133	237	123	26

Total counts of Fluoro-Jade B positive cells by section[1] and region[2] for each brain with appreciable damage at 4 days. Rats were dosed with either nitrophenyl isopropyl methyl phosphonate (NIMP) 0.6 mg/kg or paraoxon (PXN) 0.8 mg/kg subcutaneously with some receiving Oxime 20 (OX20), Oxime 15 (OX15), or pralidoxime (2PAM). Rats were perfused at the 4 day time point and brains were stained with Fluoro-Jade B. Regions selected for these counts were the CA1 and hilus of the hippocampus and the piriform cortex (PC). Some treatments did not produce appreciable neurodegeneration and, as such, are not represented in this table.

Table 2.4 4 Day Fluoro-Jade B Positive Brains – by Treatment Group

Section[1]	Region[2]	NIMP .6	PXN .8	PXN .8 +2PAM
-2.8	CA1	11	22	12
	HILUS	26	84	42
	PC	73	114	43
-3.6	CA1	48	11	7
	HILUS	13	64	36
	PC	74	123	58
-4.12	CA1	116	14	4
	HILUS	13	67	26
	PC	67	185	75

Average number of Fluoro-Jade B counts by treatment group for 4 day animals with appreciable damage by section[1] and region[2]. For all groups n=2. Rats were dosed with either nitrophenyl isopropyl methyl phosphonate (NIMP) 0.6 mg/kg or paraoxon (PXN) 0.8 mg/kg subcutaneously with some receiving Oxime 20 (OX20), Oxime 15 (OX15), or pralidoxime (2PAM). Rats were perfused at the 4 day time point and brains were stained with Fluoro-Jade B. Regions selected for these counts were the CA1 and hilus of the hippocampus and the piriform cortex (PC). Some treatment groups did not produce appreciable neurodegeneration and, as such, are not represented in this table.

CHAPTER III

MAP KINASE GENE EXPRESSION CHANGES BY NIMP AND OXIME 1

3.1 Introduction

Organophosphates are a class of chemicals of which many are used as pesticides while others have been employed in chemical warfare and terrorist attacks. They act as anticholinesterases leading to a variety of signs of cholinergic toxicity including typical nicotinic and muscarinic signs including seizures and death. Their high toxicity makes it important to have effective drugs to use in response to human exposure. Current first-line therapy in the U.S. consists of the anticholinergic atropine and the pyridinium oxime pralidoxime (2-PAM). 2-PAM acts by reactivating inhibited acetylcholinesterase (AChE) but is unable to cross the blood brain barrier. It is therefore effective at increasing survival rate of those exposed but does not effectively prevent damage to the brain due to seizure activity.

A series of novel pyridinium oximes with the potential to penetrate the blood brain barrier have been developed by Dr. Howard Chambers at Mississippi State University. Studies have been performed using a rat model to research the ability of these compounds to reactivate AChE inhibited by a non-volatile surrogate that inhibits AChE with the same chemical moiety as sarin, nitrophenyl isopropyl methylphosphonate (NIMP) (Meek et al., 2012). These studies show that these compounds are able to produce survival rates comparable to or better than 2-PAM and attenuate seizure like behavior (Chambers et al., 2016). It is therefore believed that these oximes may have the

potential to prevent brain damage in those exposed to high levels of organophosphates while also producing survival rates comparable to or better than 2-PAM.

Studies exploring the changes in biological pathways that result from exposure to OP CWAs have been performed to examine RNA expression in animal models of OP exposure. Dillman et al. (2009) demonstrated changes in gene expression in the hippocampus of soman exposed rats beginning at 1 hour and persisting for 7 days post-exposure. Spradling, Lumley, Robison, Meyerhoff, and Dillman (2011) selected the rat piriform cortex of seizing rats for examination of how sarin affects the transcriptional profile based on this region's propensity to show significant acute tissue pathology following OP induced seizures. In this study, they documented a strong upregulation in genes of inflammation and also saw changes in the mitogen-activated protein kinase (MAP kinase, MAPK) system and metabolic pathways over a period of 24 hours. Work by this same group compared gene expression of non-seizing and seizing rats exposed to sarin, demonstrating differential regulation. Of note, they observed differences in MAP kinase regulation, where apoptosis was promoted in seizing rats while inflammation was suppressed in non-seizing rats (Te, Spradling-Reeves, Dillman, & Wallqvist, 2015). Blanton, D'Ambrozio, Sistrunk, and Midboe (2003) were able to demonstrate expressional changes in diverse genes within the hippocampus and cerebral cortex following chronic low dose exposure to VX.

To further understand the physiological response of the CNS to administration of the nerve agent surrogates and treatment with novel oximes, it was decided to explore gene regulation changes resulting from exposure to these compounds. The piriform cortex was chosen for examination as this region has been cited as a region susceptible to

nerve agent induced damage. The MAP kinase system was selected as the genes of interest for this study. These genes code for proteins that belong to a large group of serine/threonine kinases that regulate cellular responses to a wide array of signals and provide for a variety of responses including inflammation and cell differentiation, proliferation, and death. They achieve these changes by phosphorylating other intracellular proteins at serine/threonine amino acids. (Hommes, Peppelenbosch, & van Deventer, 2003).

Activation of MAP kinases requires phosphorylation of both a threonine and a tyrosine by dual specificity kinases known as MAP/ERK kinases (MEKs) or MAP kinase kinases (MAPKKs). MEKs specifically phosphorylate Thr-Xxx-Tyr motifs of other proteins with the X member providing further MAP kinase pathway specificity by MEKs. As a product of this specific nature, extracellular regulated protein kinase (ERK) is only activated by MKK1 and MKK2, c-Jun N-terminal kinases (JNK) by MKK4 and MKK7, and p38 MAP kinase by MKK3, MKK4, and MKK6. Likewise, MEKs are controlled by phosphorylation by specialized enzymes called MAP kinase kinase kinases (MAPKKKs or MEKKs) (Hommes et al., 2003).

The three groups of MAPKs noted in the previous paragraph, ERK, JNK, and p38, constitute three independent MAP kinase cascades each with specific members and outcomes.

The ERK signal pathway controls cellular growth, proliferation, and survival and mediates several inflammatory processes including T cell activation. ERK has two isoforms ERK1 and ERK2 (also termed p44 and p42 respectively). These enzymes are ubiquitously expressed and are activated by MEK1 and MEK2, which are activated by

Raf. Duration of their activation is dependent upon regulatory dephosphorylative mechanisms. ERK1/2 is able to act upon both transcription factor and membrane and cytoplasmic proteins. One of their most important targets is the activating protein 1 (AP-1) transcription factors, including c-Jun, c-Fos, and activating transcription factor 2 (ATF-2). ERK1/2 also phosphorylates Elk-1, another activator of c-Fos (Hommes et al., 2003).

The JNK pathway is activated in response to cellular stress and serves to regulate cell proliferation and apoptosis. JNK proteins have at least 10 isoforms encoded by splicing of the genes JNK-1, JNK-2, and JNK-3 (RamaRao, Waghmare, Srivastava, & Bhattacharya, 2010). Similar to ERK1/2, JNK is an activator of AP-1, primarily c-Jun and ATF-2. It is activated by MKK7, in response to cytokines, and MKK4, in response to environmental stress. Upstream activators of these MAPKKs include more than 12 intracellular proteins including MEKK1-4. There are four known negative regulators of JNK: MAP kinase phosphatase MKP7, heat shock protein 72 (HSP72), Evil onco-protein, and nitric oxide. JNK signaling is thought to play a role in many pathological conditions such as cancer, stroke, heart disease, and inflammatory disorders (Hommes et al., 2003).

The p38 pathway is another mediator of inflammation and cell growth, proliferation, and death. In regard to inflammation, p38 affects inflammatory mediators of leukocyte recruitment and activation. This includes E-selectin and VCAM1 mediated rolling adhesion of leukocytes and endothelial cells and regulation of TNF-α synthesis. There are four identified isoforms, two of which (p38α and p38β) are expressed ubiquitously. p38 is primarily activated by various cytokines but can also activate in response to activation of Toll-like receptors by pathogens. Its upstream activators are

MKK3, MKK4, and MKK6. Upon activation, p38 phosphorylates either other kinases of transcription factors such as ATF-2 or myocyte enhancer factor 2 (MEF2). p38 is a potential activator of NF-κB transcription (Hommes et al., 2003).

While the MAP kinase system has three separate pathways, there is potential for upstream and downstream interactions between the three. Some upstream activators, such as p21Rac, may simultaneously activate more than one MAPK pathway. On the other end of the pathway, some targets of MAP kinase proteins can act as either kinases or phosphatases providing either activation or deactivation of other MAPK enzymes (Hommes et al., 2003).

Other groups have previously investigated the effects that OPs have on MAP kinase activation. Niijima et al. (2000) were able to display an increase in phosphorylation state of JNK, phospholipase C γ (PLC γ) and cytosolic MAPK following treatment of rats using LD_{50} dosages of sarin and soman nerve agent surrogates. RamaRao et al. (2010) demonstrated increases in the phosphorylation of JNK3 and calcium/calmodulin-dependent protein kinase II (CaMKII) of the cerebrum, hippocampus, and thalamus beginning 2.5 hours after soman administration and continuing until 30 days post-exposure. Damodaran et al. (2006) showed changes in expression of many diverse genes in brains of rats exposed to sarin both 15 minutes and 3 months after treatment. These included Camk1b, Camk2d, Map2k, CamkIIa, Jun, and Fos. This study demonstrated changes in many other genes affecting cytokines, neurotransmission, cell signaling, ion channels, cell cycle, apoptosis, and cell metabolism.

By studying changes in MAP kinase gene regulation it was hoped to better understand how the brain responds to the nerve agent surrogates and potentially show a sparing effect on these changes when novel oxime treatment is provided. It was expected that the sarin surrogate NIMP would produce alterations of MAP kinase gene expression and treatment with the novel oximes would return gene expression to levels closer to baseline.

To study this gene expression, a standard qPCR kit developed specifically for expression of this gene system within rats was used. The Qiagen RT^2 Profiler PCR Array MAP Kinase Signaling Pathway kit was used with the associated sample preparation kits in order to guarantee sample consistency and compatibility with the qPCR assay. The novel oxime chosen for this study was Oxime 1, which has been one of the most promising oximes in studies up to this point (Chambers et al., 2016).

3.2 Methods

3.2.1 Treatments

Treatments for these animals were performed as previously described (Chambers et al., 2013). Adult male (250-300g) Sprague Dawley rats were injected subcutaneously with either a high sublethal dosage of the sarin surrogate NIMP (0.325 mg/kg) or vehicle (DMSO). One hour after injection, which should represent time of peak brain AChE inhibition of about 80%, rats were administered an intramuscular injection of either 146 μmol/kg (the human equivalent dose) of the novel Oxime 1 or vehicle (Multisol). Rats were sacrificed 2 hours later and the piriform cortices quickly dissected, placed in an RNAse free tube, and frozen in liquid nitrogen. Samples were stored at -80°C until total

RNA extraction. Three brains were collected for each of the following treatments: vehicle control, Oxime 1 control, NIMP, and NIMP plus Oxime 1.

3.2.2 RNA Isolation

Total cortex RNA was isolated using Qiagen's RNeasy® Plus Mini Kit (Valencia, CA) per manufacturer's instructions. Samples were homogenized in individual tubes on ice with RNAse free plastic grinders. Lysates were centrifuged through QIAshredder columns to ensure complete tissue disruption followed by centrifugation through gDNA eliminator columns to remove genomic DNA. Purity and concentration of the RNA samples were determined by 260/230 and 260/280 absorbance ratios measured with a Nanodrop ND-1000 spectrophotometer. Samples with concentrations higher than 40 ng/µl and an 260/230 absorbance ratio greater than 1.7 were suitable for use and examined on bleach agarose gels for integrity of both the 28S and 18S RNAs by the method described in Aranda, LaJoie, & Jorcyk (2012).

3.2.3 Reverse Transcription

cDNA was reverse transcribed using Qiagen's RT^2 First Strand Kit. 0.5µg of isolated RNA was processed according to the manufacturer's instructions for each 96 well plate PCR array. A genomic DNA elimination buffer was used prior to reverse transcription to eliminate any remaining genomic DNA. RE3 reverse transcripase mix was primed in an unbiased manner with random hexamers and oligo-dT primers. Samples were stored at -20^{o}C until performing real-time qPCR.

3.2.4 Real-Time qPCR

Real-time qPCR was performed using Qiagen's RT² Profiler™ PCR Array Rat MAP Kinase Signaling Pathway (Qiagen Product no. 330231, Cat. no. PARN-061Z), a 96 well plate containing primer assays for 84 rat MAP kinase genes, 5 housekeeping genes, 3 reverse transcription controls, 3 positive PCR controls, and one genomic DNA control arranged as seen in Figure 3.1 (Qiagen, 2011). cDNA was combined with Qiagen RT^2 SYBR Green ROX™ qPCR Mastermix and 25µl were dispensed into each well. Plates were amplified on a Stratagene Mx3005P® real-time cycler.

3.2.5 Data Analysis

CT values were calculated with Stratagene's MxPro QPCR software. Threshold was determined on the first array and kept constant on all following plates. CT values from each array were uploaded to Qiagen's GeneGlobe Data Analysis Center. The application performed quality control to ensure that all controls were within acceptable limits indicating adequate reverse transcription and PCR performance and absence of genomic DNA. The Rplp1 gene was manually selected for data normalization due to lowest variation between sample Ct values. Fold change was calculated to represent normalized gene expression as (2^(- Delta Ct)). P values were calculated by Student's t-test of the fold change values. These data were used to generate scatter and volcano plots, heat maps, and multigroup plots for differential analysis among treatment groups.

3.3 Results

Twelve rats were treated following the protocol described above with three rats in each treatment group. Their piriform cortices were harvested, and total RNA was isolated while DNA was eliminated. All RNA met the quality control standards as described in the user manual: 260/280 absorbance ratio greater than or equal to 2, 260/230 absorbance ratio of greater than or equal to 1.7, 40 ng/µl, and well defined 28S and 18S RNA band on bleach agarose gel electrophoresis. Reverse transcription of RNA to cDNA was performed and qPCR of cDNA was performed using the provided arrays. All raw data looked acceptable based on low background signal and acceptable melting curve appearance. Raw data were compiled and loaded into the Qiagen Data Analysis Center. All samples met the application's quality control standards, and the Rplp1 gene was selected for normalization of data between plates.

From analysis of qPCR arrays, data for 84 genes of interest were generated for each animal in this study.

In comparing the vehicle control group to the Oxime 1 control group, most of the genes displayed very little to no change. Fold changes of interest were Map4k1 0.38, Mos 0.58 p=0.048, and Sfn 0.24 as shown in Table 3.1.

Comparing vehicle control to the NIMP treated group showed more differences in fold gene expression changes. Most notable are Ccna2 2.68 p=0.044, Cdkn1a 2.44, and Cdkn2a 0.12 p=0.041 (Table 3.1). An additional 9 genes displayed a fold change of less than 0.5 but were not statistically relevant.

When the NIMP + Oxime 1 treated group is compared to vehicle, there appear to be less genes whose expression was altered than seen with NIMP treatment alone. The

only fold changes of note are: Kcnh8 0.26, Map4k1 0.38, Mos 0.26 p=0.006, and Sfn 0.35 (Table 3.1). The fold change of these genes of interest are displayed in Figure 3.2.

3.4 Discussion

The data generated in this study demonstrate that the sarin surrogate NIMP is able to elicit changes in transcriptional regulation of the MAP kinase system within the piriform cortices of rats administered a sublethal dose. These data also show that rats treated with Oxime 1 alone have few alterations in the expression of genes within the MAP kinase cascade. When this oxime is given in conjunction with NIMP, it attenuates many of the changes seen with NIMP alone. Perhaps more importantly, this study identifies the genes whose expression is altered by these compounds. These observations can therefore give insight as to what physiologic responses might be elicited by these compounds.

3.4.1 Oxime Treatment

The only genes that displayed notable changes in expression by Oxime 1 alone were Map4k1, Mos, and Sfn.

3.4.1.1 Map4k1

Map4k is also known as hematopoietic progenitor kinase 1 (HPK1). It is primarily expressed in hematopoietic organs and cells and acts in many signal systems including MAP kinase, antigen receptors, apoptosis, growth factors, and cytokines. It can also serve as a connection between surface receptors and JNK signaling. It can be activated by stimulation of various receptors including T or B cell antigen receptors, transforming growth factor-β receptor (TGF-βR), erythropoietin receptor, Fas, and E

prostanoid receptor (Li, Han, Chen, Yu, & Zhang 2008a). It has been shown in a rat stroke model that MAP4k1 is upregulated and knocking down MAP4k1's activity provides neuroprotection by decreasing activation of the MLK3-MKK7-JNK3 pathway (Li, Yu, & Zhang 2008b). Another study by the same group demonstrated that inhibition of Src kinase activation either by direct inhibition of Src or inhibition of NMDA receptors decreases phosphorylation of MAP4k1, MLK3, JNK, and c-Jun. Inhibition of this pathway provided neuroprotection when subsequent experimental cerebral ischemia was performed (Li et al., 2008a). Work by Lasserre et al. (2011) provided evidence that MAP4k1 is a regulator of T cell response intensity by inducing 14-3-3 protein binding that release the signaling adaptors SLP76-GADS from the membrane reducing induced gene transcription.

Considering these observations, it is possible that the decrease in Map4k1 expression invoked by Oxime 1 could have a neuroprotective role by ultimately decreasing JNK activation. Another possibility is that through impairment of T cell activation within the CNS, the brain's response to damage might be altered. While the CNS is generally considered to be immunologically privileged, there is growing evidence that T cells are both present and important in the normal function of the CNS and in its response to stressful stimuli. Studies using mouse hippocampal slices exposed to kainic acid have demonstrated that the presence of $CD4^+$ and $CD8^+$ T cells improve neuronal survival and reduce p38 and ERK activation likely through activation of astrocytes by IFN-γ and IL-4 (Ellwardt, Walsh, Kipnis, & Zipp, 2016). It is possible that by decreasing T cell activation, Oxime 1 could decrease the brain's ability to properly respond to excitotoxic neuronal stress.

3.4.1.2 Mos

The next gene altered by Oxime 1 was Mos, the Moloney sarcoma oncogene. Most studies to date have concentrated on the function of Mos with regard to meiotic cells. Mos functions as an upstream activator of MAP2K1 and MAP2K2 (MEK1/2), which are upstream activators of ERK 1 and ERK2 (Gonzalez-Garcia et al., 2014). Depending on how ERK1/2 are activated, they can promote many cellular functions including proliferation, cell survival, and cell death (Mebratu & Tesfaigz, 2009). During the final stages of oocyte maturation Mos synthesis is upregulated leading to a downstream upregulation of the MAP kinase pathway, which promotes maturation of the oocyte (Gonzalez-Garcia et al., 2014). Perrard, Chassaing, Montillet, Sabido, and Durand (2009) identified Mos in male meiotic cells where they noted a positive feedback between MAP kinase and Mos. Their findings suggested a relationship between an increase in Mos and a β-NGF induced cell cycle arrest. Kalejs et al. (2006) noted upregulation of Mos and several other genes that the authors considered meiosis specific in p53 mutated lymphoma cell lines. They suggested that increased Mos protein concentrations could play a role in the metaphase arrest of mitotic catastrophe.

Despite little data on the function of Mos outside of the meiotic cell, some inferences could be made towards what effects its downregulation may mean in the cells of Oxime 1 treated animals. As Mos is an upstream activator of MEK1/2, decreased Mos expression could lead to less overall MAP kinase activation down this pathway. While mode of activation of MEK1/2 and ERK1/2 can affect the physiological outcome that these enzymes promote, decreased Mos expression would likely be less detrimental than increased expression. An increase would more likely promote cell death while a decrease

might indicate cellular stasis. It is possible that decreased activation of MEK1/2 and ERK1/2 could decrease signaling for apoptosis.

3.4.1.3 Sfn

Sfn codes for the protein 14-3-3σ, a member of the 14-3-3 protein family. These proteins are known to be present primarily in the brain tissue of animals contribute to neuron function. The first identified function of these proteins was as an activator of tyrosine hydroxylase and tryptophan hydroxylase, enzymes responsible for the production of neurotransmitters (Ferl, Manak, & Reyer, 2002). This 14-3-3 protein is termed tyrosine hydroxylase/tryptophan hydroxylase activation protein (Furukawa et al., 2011). They have also been detected in extracellular environments such as the cerebrospinal fluid (Hermeking, 2004). 14-3-3s can interact with ASK1 to inhibit apoptosis (Kim, Khursigara, Sun, Franke, & Chao, 2001). Structurally these proteins have a highly conserved core region that serves as the proteins' functional region and divergent amino and carboxyl termini. Ligands to which the core region binds are often phosphorylated at a serine or threonine residue in the target sequence, but this is not always the case. Another protein in the MAP kinase cascade, Raf-1, is also a 14-3-3 protein (Ferl et al., 2002).

14-3-3σ expression was initially observed in differentiating epithelial cells where its expression is induced when keratinocytes are exiting the stem cell compartment (Hermeking, 2004). More than 100 ligands have been identified for this protein affecting many cellular processes including cell proliferation, cell cycle regulation, and apoptosis. Its expression is regulated by p53 and BRCA1 (Li, Liu, & Zhang, 2009). Exogenous expression of this protein results in inhibited G2/M progression. The mechanism of 14-3-

3σ G2 arrest in cases of DNA damage begins with Rad3-dependent activation of Chk1 kinase, which phosphorylates Ser-216 of Cdc25C phosphatase. This phosphorylated serine serves as a binding site for 14-3-3σ. Binding of Cdc25C sequesters this enzyme out of the nucleus preventing it from dephosphorylating Cdc2, a cyclin-dependent kinase required for entry into mitosis. DNA damage has been shown to increase p53 mediated upregulation of 14-3-3σ, and exogenously delivered p53 produced a pronounced increase of Sfn RNA. Several indicators support that experimentally increased 14-3-3σ protein concentration produces a G2 arrest. This cell cycle block can be uncoordinated with DNA synthesis proceeding between mitoses. It is thought that this loss of coordination might be due to lack of p21 modulation. In cases of DNA damage both 14-3-3σ and p21 are activated with p21 preventing DNA synthesis through inhibition of cyclin-dependent kinases (Hermeking et al., 1997). Epigenetic suppression of Sfn is seen in many carcinomas giving rise to the belief that it is a tumor-suppressive gene. Experimental removal of this gene removes the ability of cells to maintain a stable G2/M arrest following DNA damage (Hermeking, 2004). Evidence also exists for post-transciptional regulation of 14-3-3σ, possibly a product of mRNA stability, translational efficiency, and protein stability. This leads to the assumption that regulation of 14-3-3σ takes place at multiple levels (Li et al., 2009). In human gliomas, the degree of Sfn expression downregulation has been correlated with disease prognosis (Deng et al., 2011).

In Oxime 1 treated animals, the fold change in Sfn expression decreased to 0.58. This could indicate that Oxime 1 might alter some of the normal functions of neurons such as production of neurotransmitters. This could potentially alter the amount of neurotransmitter available to continue neuronal signals. It is possible that this could be

protective in the face of excitotoxicity. The lack of 14-3-3σ could be detrimental in cellular response to damage and could promote either development of neoplasia or continuance through the cell cycle promoting apoptosis.

3.4.2 NIMP Treatment

More genes were altered by NIMP administration than Oxime 1. Of most interest were Ccna2, Cdkn1a, and Cdkn2a. Contrary to what was seen in Oxime 1 treated animals, Mos was observed to increase with NIMP alone treatment.

3.4.2.1 Ccna2

NIMP treatment significantly increased Ccna2 levels by 2.68 fold. Ccna2 (cyclin A2) serves to regulate cell cycle at mitosis and interphase by interacting with cyclin-dependent kinases 1 and 2 (Cdk1 and Cdk2). Most cyclin A2 is degraded either by the ubiquitin system or by autophagy before mitosis occurs. This is necessary for alignment of chromosomes and progression into anaphase (Loukil et al., 2016). Additionally, cyclin A2 promotes activation of Rho signaling molecules that control cell morphology, motility, and cytokinesis. In the absence of cyclin A2, RhoA activity decreases producing increased cell motility and invasiveness. Increased RhoA is necessary at the end of mitosis in order to form the cleavage furrow. It localizes at the poles of the furrow while the remaining cyclin A2 aligns between these poles across the cleavage furrow (Loukil et al., 2016). This protein also serves as a regulator of G1 to S phase transition in the cell cycle as well as G2 to M (Fung, Ma, & Poon, 2007; Gygli et al., 2016). Knockdown of Ccna2 expression delays entry into mitosis. Cyclin A cannot drive mitosis by itself and requires cyclin B to push the cell into mitosis (Fung et al., 2007). Cyclin A2 has also been implicated in DNA damage response. It can be found located at sites of DNA double-

strand breaks serving for repair of the break either through homologous recombination or non-homologous end joining. Mice lacking cyclin A2 had deficient repair of neuronal DNA (Gygli et al., 2016). Cyclin A2 overexpression can cause premature entry and prolongation of S phase as well as induce double strand breaks of the DNA (Tane &Chibazakura, 2009). A study by Seidel et al. (2011) showed that Ccna2 gene expression increases in a rat cerebral ischemia model, likely as a result of decreased promyelocytic leukemia zinc finger (PLZF) protein levels. A study of gene expression in a rodent spinal cord model by Wu et al. (2014) showed that cyclin genes such as Ccna2 show increased expression in the cerebral cortex and hippocampus.

The increase seen in Ccna2 as a product of NIMP administration could have several potential explanations. One of the more likely would be that the stresses the neurons face from increased cholinergic stimulation and seizure activity could lead to perturbations of the cell cycle including: neurogenesis, increased cell cycle, or apoptosis. Another possibility could be that the OP might induce DNA damage to which Ccna2 synthesis is increased in response.

3.4.2.2 Cdkn1a

Cdkn1a gene expression was also elevated following NIMP administration. This gene encodes a protein, p21, that inhibits cyclin/cyclin-dependent kinase (CDK) complexes helping to regulate cell-cycle transitions. It is able to interact with almost any CDK complex. Its mechanism is not always inhibitory and in some cases such as CDK4/6 it can even be stimulatory. It can also target molecules other than CDKs including MEKK5 and CK2 kinases, calmodulin, GADD45, procaspase 3, and oncogenic protein SET. By binding proliferating cell nuclear antigen (PCNA) Cdkn2a can interfere

with DNA replication. Cdkn2a can also affect transcription by inhibiting E2F, Myc, and STAT3 or stimulating NFκB –mediated transcription. p21 expression is increased in different cells by stress stimuli such as DNA damage, agents that affect DNA synthesis or mitosis, TGFβ, and differentiating or oncogenic chemicals (Roninson, 2002). It is considered to be the primary mediator of G_1 arrest due to DNA damage. It is also important in the G_2-phase checkpoint as well (Cazzalini, Scovassi, Savio, Stivala, & Prosperi, 2010). Cdkn1a increase is due to changes in transcriptional activation and mRNA and protein stability. This increase is transient indicating that p21 is likely only involved in the early stages of cell cycle arrest. Cdkn1a, along with Cdkn2a and p53, is involved in accelerated cellular senescence induced by DNA damage or telomere shortening (Roninson, 2002) Both Cdkn1a and Cdkn2a are upregulated in response to aberrant mitotic progression (Dikovskaya et al., 2015).

One major function of Cdkn1a is as an anti-apoptotic factor. This is due to interactions with several molecules including: binding procaspase 3 to prevent its conversion to caspase 3, interacting with caspases 8 and 10, inhibiting apoptosis-regulating kinases, and inhibiting apoptosis-stimulating kinases Myc and E2F. It is cleaved by caspase 3 at the beginning of apoptosis to remove this suppression (Roninson, 2002). Other sources have reported that p21 can serve in a pro-apoptotic role as well. Cell models that over express p21 directly or through increased p53 activation of p21 induce apoptosis. p21-null primary hepatocytes have also been shown to display less apoptosis when challenged than wild-type (Liu, Bishop, & Liu, 2003). In one study with squamous carcinoma cells mutated to overexpress p21, this protein was shown to either be pro- or anti-apoptotic depending on which chemotherapeutic was administered. Subcellular

localization likely plays a part in this differential action. Cytoplasmically p21 can block activation of caspase and pro-apoptotic MAP kinase proteins, but inside the nucleus it favors apoptosis due to DNA damage (Cazzalini et al., 2010).

As mature neurons maintain a quiescent state throughout their life, alteration of their cell cycle regulation can be detrimental. Reentry into the cell cycle by mature neurons is associated with cell death. In Alzheimer's disease models, re-expression of cell cycle genes is seen prior to neuronal death. This alteration in cell cycle machinery does not appear to be sufficient for neuronal death but may be a priming event for neurodegeneration (Kawauchi, Shikanai, & Kosodo, 2013).

Due to the diverse nature of p21 as a cellular regulator, interpretation of increased Cdkn1a gene expression is difficult. Given the static nature of mature neurons, any alteration of cell cycle machinery is likely detrimental. If nothing else, the change in p21 regulation could serve as a primer for neurodegeneration or neurodegenerative diseases. It could be that Cdkn1a is upregulated to either serve as an apoptosis inducer or in an attempt to prevent cellular apoptosis. Finally, it is possible that NIMP could be causing DNA damage either through direct interaction or cellular stress, and this is promoting an upregulation in Cdkn1a in response.

3.4.2.3 Cdkn2a

Like Cdkn1a, Cdkn2a codes for a CDK inhibitor, p16. It acts as a negative regulator of cell cycle (Zhao, Choi, Lee, Bode, & Dong 2016). Binding of p16 to CDK4 or CDK6 prevents these proteins from complexing with cyclin D interfering with this controller of G1 phase proliferation (Serrano, Hannon, & Beach, 1993). Lack of the CDK6/4-cyclin D complex promotes G1 arrest through lack of the Rb/E2F complex

(Zhao et al., 2016). In astrocytes, increased p16 expression is observed in cellular senescence and may be a contributor to Alzheimer's disease (Bhat et al., 2012).

p16 additionally serves as a potential tumor suppressor and its inactivation is increasingly seen with the advancing stages of cancer progression (Zhao et al., 2016). Methylation of Cdkn2a is frequently seen in myelodysplastic syndrome. This methylation was correlated with levels of cellular oxidative stress in the form of reactive oxygen species (Goncalves et al., 2016). Inactivation of Cdkn2a is a common feature of non-small-cell lung cancer resultant of smoke exposure (Tam et al., 2013). Astrocytic gliomas also underexpress Cdkn2a among other cell cycle genes with progressively more deregulation with increasing tumor grade (Ferreira et al., 2015). Similarly, suppression of Cdkn2a and other cell cycle genes was observed in meningiomas (Bostrom et al., 2001).

In a cerebral ischemia model, p16 was observed to be downregulated in neurons following ischemia and reperfusion. By using multiple labels for p16, MAP-2, and TUNEL, researchers were able to show that at 9 hours after ischemia p16 staining decreases even before any TUNEL labeling becomes apparent. As time progressed, TUNEL labeled cell numbers increased while the number of intact p16 negative cells decreased. At 72 hours, all remaining morphologically intact MAP-2 labeled cells were p16 positive. This study supports that p16 regulation precedes neuronal cell death (Katchanov et al., 2001).

Cdkn2a encodes an alternate open reading frame that produces the protein p19 that interacts with the p53 pathway (Zhao et al., 2016). p19 helps to coordinate the self-renewal and determination of neuronal and glial fate of neuronal stem cells. Inactivation

or forced expression of p19 can alter the stage of these cells, changing their functions and fates (Nagao et al., 2008).

In this model, treatment with NIMP produces a significant decrease in Cdkn2a expression. Decrease in Cdkn2a expression removes inhibition on CDK complexes promoting cell cycle. Reentry of mature neuronal cells into the cell cycle leads to cell death, and as noted above, decreased p16 expression has been implicated as a preceding event to apoptosis. Alternate interpretations could be that changes to the astrocyte population resulting from NIMP exposure could resemble the changes that occur during senescence that would be mediated by p16. Additionally, Cdkn2a transcription could be for p19. In that case, the seizure activity generated by NIMP could be promoting neurogenesis from the stem cell population and therefore calling for changes in p19 regulation.

3.4.2.4 Mos

The physiology of Mos has been described earlier in this chapter. As opposed to Oxime 1, NIMP provided for an increase in Mos expression. With Mos being an upstream activator of MEK1/2 and ERK1/2, this increase will most likely promote signaling down this pathway. Activation of this pathway has various outcomes including cell proliferation, cell survival, and cell death. It is possible that Mos activation could be a compensatory mechanism to promote cell survival in the face of excitotoxicity. Alternately it could be promoting reentry into the cell cycle of mature neurons and cellular apoptosis.

3.4.3 NIMP + Oxime 1 Treatment

Oxime 1 treatment following NIMP produced a return toward baseline in several of the genes whose expression had been altered by NIMP, Ccna2, Cdkn1a, and Cdkn2a. It also mirrored the changes in Map4k1, Mos, and Sfn that were seen by Oxime 1 alone treatment. Additionally, Kcnh8 and Kcnn1 showed alterations more extreme than either NIMP or Oxime 1 alone.

3.4.3.1 Ccna2

In rats treated with NIMP and Oxime 1, Ccna2 is not upregulated as with NIMP treatment alone. Its expression is close to that of the control. This likely indicates that the alterations of cell cycle such as neurogenesis or apoptosis caused by NIMP treatment are not seen in animals that also receive Oxime 1 therapy. This promotes the view that Oxime 1 is protective against NIMP exposure.

3.4.3.2 Cdkn1a

While Cdkn1a was not significantly upregulated in the NIMP alone treated rats, its mean was more than two times that of control. With Oxime 1 treatment, this value returned to much closer to baseline. Due to the multitude of processes regulated by Cdkn1a, it is difficult to predict what changes that NIMP produced that Oxime 1 might be affecting. It does demonstrate that Oxime 1 attenuates some responses of the rat brain to NIMP administration.

3.4.3.3 Cdkn2a

Unlike the previous genes, the transcription of Cdkn2a was significantly decreased by NIMP administration. Oxime 1 treatment in addition to NIMP returns this value to closer to baseline. As decrease of this CDK inhibitor promotes entry into the cell cycle, the return towards baseline likely indicates that Oxime 1 treatment is lessening the stimulation of mature neurons to reenter the cell cycle. This would mean these cells are less likely to undergo neurodegeneration promoting the theory that Oxime 1 therapy is protective against OP induced neuronal damage.

3.4.3.4 Map4k1

As with Oxime 1 alone treatment, Oxime 1 + NIMP treated animals still see a similar decrease in Map4k1 when compared to control. It is likely that this depression could be neuroprotective through suppression of JNK activation.

3.4.3.5 Mos

When NIMP and Oxime 1 are administered together, expression of Mos significantly decreases, even more so than when only Oxime 1 is given. The reason for this additive effect is not readily apparent as NIMP alone produces an increase in Mos expression. The decrease in Mos will lessen activation of MEK1/2 and ERK1/2, which might promote cellular stasis. This stasis might be neuroprotective in the fact of excitotoxicity induced by NIMP.

3.4.3.6 Sfn

Oxime 1 + NIMP treated animals demonstrate a similar decrease in Sfn to Oxime 1 treated rats. This indicates Oxime 1, whether with or without NIMP treatment produces some similar changes in the normal function of the cells, which could be potentially detrimental to survival.

3.4.3.7 Kcnh8

Kcnh8 saw a decrease in expression following administration of both NIMP and Oxime 1 while not being as strongly affected by either compound alone. Kcnh8 encodes for elk, a subfamily of the EAG family of potassium channel pore-forming subunits. All of the known members of this family form potassium channels that function at either subthreshold or near threshold voltages. Some of these channels are always active and can contribute to steady outward currents during long depolarizations. Even those that are able to inactivate, a portion of their current never inactivates. Aside from elk, there are two other EAG subfamilies, eag and erg. Subunits of these subfamilies are only able to interact with subunits of the same family producing heteromultimeric channels with various functional properties. This variety of channels produces an M-like current that is a complex combination of ion channels (Saganich, Machado, & Rudy, 2001).

By decreasing Kcnh8 expression, NIMP and Oxime 1 could produce alterations in the membrane excitability of neurons. While unlikely to produce changes severe enough to affect excitotoxicity, the potential changes to resting neuron voltage and length of depolarization, could alter mental capacity and behavior in those exposed.

3.4.3.8 Kcnn1

Kcnn1 also decreased more when rats were treated with both NIMP and Oxime 1 than with either compound alone. Kcnn1 codes for SK1, a member of the SK family of calcium-activated potassium channels. SK1 alone is not able to form functional homomeric units (D'hoedt, Hirzel, Pedarzani, & Stocker, 2004). When SK1 and SK2 are both expressed, current magnitude is increased, and the channels are less sensitive to blocking agents indicating a functional interaction between these two subunits (Benton et al., 2003) In a neurotoxic model of Parkinson's disease, increased neuronal firing was associated with an increase in SK channel activity. Neurotoxicity in this model was indicated to be a product of SK channel changes (Wang et al., 2015).

While Kcnn1's product, SK1, does not form a functional channel on its own, it is able to interact with related subunits to form potassium channels able to alter the magnitude of nerve conductances. Experimental data indicate that these channels alter neuronal firing patterns and might contribute to excitotoxicity. With a decrease in expression, treatment with these compounds may lead to alterations of neural firing, which could lead to behavioral changes following treatment. Considering that expression is depressed, which would likely decrease conductance magnitude, this change could potentially be protective against excitotoxicity.

3.5 Conclusion

Examination of MAP kinase gene expression in the rat piriform cortex provides evidence that administration of both Oxime 1 and sublethal NIMP cause alterations in the transcription of several genes involved in cell signaling and the cell cycle. Additionally,

treatment of NIMP exposure with Oxime 1 was able to attenuate some of the changes in gene regulation

While Oxime 1 is intended as an antidote to organophosphate poisoning, its presence within the tissue leads to the possibility that it could have physiological effects even in the absence of these compounds. Generally the alteration of MAP kinase transcription was less pronounced in this group than the other examined treatments, but the expression of Map4k1, Mos, and Sfn were decreased with Oxime 1 treatment. Decreased Map4k1 expression could possibly be neuroprotective by decreasing activation of JNK, but it is also possible that by having lower concentrations of Map4k1, T cell activation might be impaired, potentially limiting the brain's natural response to excitotoxic stress. Mos is an upstream activator of MEK1/2 and ERK1/2. By decreasing its expression, activation of the downstream MAP kinase enzymes might be decreased with various effects dependent upon the exact mode of activation. It is possible that the decreased activation of this pathway could be neuroprotective by decreasing signaling for apoptosis. Decreased Sfn could have several potential outcomes. One of its roles is in the production of the neurotransmitters serotonin and dopamine. It is possible that the decrease in the availability of these neurotransmitters resulting from decreased Sfn expression could be somewhat protective when faced with excitotoxicity. Another possible effect would be that alterations of the cell's ability to undergo G2 arrest could promote either apoptosis or neoplasia in the absence of this normal safeguard.

The general theme of genes whose expression was altered by NIMP exposure was control of cell cycle and apoptosis. Both the observed increase in Ccna2 and Cdkn2a would suggest that neurons are being regulated into continuing through the cell cycle. In

mature neurons this would likely indicate that they were being directed towards apoptosis. In cells that are not terminally differentiated it could mean that the cells might be undergoing neurogenesis in response to cellular stress. The increase in Cdkn1a is less clear-cut as, depending on the circumstances, this regulation might either promote or hinder apoptosis. This could mean that either this regulation is assisting in promoting cell death, or alternatively, it could be a compensatory mechanism to promote cell survival. The final gene effect by NIMP alone, Mos, is an upstream regulator of MEK1/2 and ERK1/2. Since NIMP increases Mos expression, activation of these other proteins should increase producing changes in signaling for cell proliferation, cell survival, and cell death. Considering this, like Cdkn1a, Mos could have more than one function. It is possible that increased expression of this gene could promote cell survival and oppose apoptosis. It could also be that this increased expression will promote apoptosis and contribute to neurodegeneration from NIMP exposure.

When NIMP exposed rats are subsequently treated with Oxime 1, several of the genes that showed major alterations in expression returned toward baseline. These included Ccna2, Cdkn1a, and Cdkn2a. Also, like Oxime 1 alone treatment, Map4k1, Mos, and Sfn were decreased. Finally, Kcnh8 and Kcnn1, which were not changed with either NIMP or Oxime 1 alone, decreased when exposed to both compounds. The return toward baseline of Ccna2, Cdkn1a, and Cdkn2a promotes the idea that Oxime 1 is protective against NIMP induced excitotoxicity, producing less cellular signaling for entry into the cell cycle and apoptosis. Alteration of Map4k1, Mos, and Sfn regulation similar to Oxime 1 treatment alone suggests that Oxime 1 does have physiological effects of its own that are independent of its function to combat organophosphate binding of

AChE. The fact that treatment with NIMP and Oxime 1 together produces a more significant change in Kcnh8 and Kcnn1 than either compound alone suggests that these compounds can have an additive effect to alter cellular activity. As both of these genes produce potassium channels, it is likely that the change in their expression would alter membrane excitability and function possibly affecting neuronal function and behavior in the future.

The results of this study provide evidence that like CWA organophosphates, NIMP is able to produce alterations of gene expression. In all of these previous studies, MAP kinase alterations were noted (Damodaran et al., 2006; Dillman et al., 2009; Spradling et al., 2011; Te et al., 2015). By investigating MAP kinase gene expression, this study not only demonstrated that NIMP alters cellular signaling and Oxime 1 attenuates some of these changes, but also provided insight into what downstream effects might result from these changes. These data support that NIMP promotes reentry into the cell cycle, likely by promoting apoptosis, but also possibly through induction of neurogenesis as a stress response. It demonstrates that Oxime 1 is protective against this signaling while also having some physiological effects of its own and even having additive effects when given in the presence of NIMP.

Table 3.1 Fold Changes in Expression of Select MAP Kinase Genes by Treatment

Genes	Oxime 1			NIMP + Oxime 1			NIMP		
	Fold Change[1]	95% CI	P-Value[2]	Fold Change[1]	95% CI	P-Value[2]	Fold Change[1]	95% CI	P-Value[2]
Ccna2	1.278	(0.92, 1.64)	0.149	0.966	(0.00001, 2.11)	0.651	2.682	(1.35, 4.01)	**0.044***
Cdkn1a	1.478	(0.93, 2.02)	0.107	1.350	(0.80, 1.90)	0.249	2.440	(0.59, 4.28)	0.160
Cdkn2a	1.173	(0.48, 1.86)	0.528	0.573	(0.00001, 1.26)	0.744	0.117	(0.00001, 0.37)	**0.041***
Kcnh8	0.829	(0.10, 1.56)	0.698	0.257	(0.00001, 0.72)	0.146	0.599	(0.00001, 1.66)	0.932
Kcnn1	0.885	(0.53, 1.24)	0.560	0.578	(0.16, 1.00)	0.245	0.697	(0.00001, 1.56)	0.824
Map4k1	0.375	(0.00001, 0.78)	0.279	0.381	(0.00001, 0.81)	0.285	0.611	(0.00001, 1.42)	0.473
Mos	0.584	(0.38, 0.79)	**0.048***	0.259	(0.14, 0.38)	**0.006***	1.753	(0.00001, 3.58)	0.367
Sfn	0.235	(0.00001, 0.65)	0.239	0.350	(0.00001, 0.89)	0.261	0.818	(0.00001, 2.50)	0.824

Data on fold change of MAP kinase genes relative to vehicle control for all other treatments. Fold change was calculated to represent normalized gene expression as (2^(- Delta Ct))[1]. P values were calculated by Student's T-Test of the fold change values relative to vehicle controls[2].

	1	2	3	4	5	6	7	8	9	10	11	12
A	Araf	Atf2	Ccna1	Ccna2	Ccnb1	Ccnb2	Ccnd1	Ccnd2	Ccnd3	Ccne1	Cdc42	Cdk2
B	Cdk4	Cdk6	Cdkn1a	Cdkn1b	Cdkn1c	Cdkn2a	Cdkn2b	Cdkn2c	Cdkn2d	Chuk	Col1a1	Creb1
C	Crebbp	Dlk1	E2f1	Egfr	Egr1	Ets1	Ets2	Fos	Grb2	Hras	Hspa5	Hspb1
D	Jun	Kcnh8	Kcnn1	Kras	Ksr1	Map2k1	Map2k1pi1	Map2k2	Map2k3	Map2k4	Map2k5	Map2k6
E	Map2k7	Map3k1	Map3k2	Map3k3	Map3k4	Map4k1	Mapk1	Mapk10	Mapk11	Mapk12	Mapk13	Mapk14
F	Mapk3	Mapk6	Mapk7	Mapk8	Mapk8ip1	Mapk8ip2	Mapk8ip3	Mapk9	Mapkapk2	Mapkapk5	Max	Mef2c
G	Mknk1	Mos	Myc	Nfatc4	Nras	Pak1	Rac1	Raf1	Rb1	Sfn	Smad4	Tp53
H	Actb	B2m	Hprt1	Ldha	Rplp1	RGDC[1]	RTC[2]	RTC[2]	RTC[2]	PPC[3]	PPC[3]	PPC[3]

Figure 3.1 Layout of Gene Primers of Qiagen RT2 Profiler Rat MAP Kinase PCR Array

Arrangement of genes on the Qiagen RT2 Profiler Rat MAP Kinase PCR Array. RGDC tests for any remaining genomic DNA[1]. RTC tests the efficiency of the reverse-transcription reaction[2]. PPC tests for the efficiency of the PCR reaction[3].

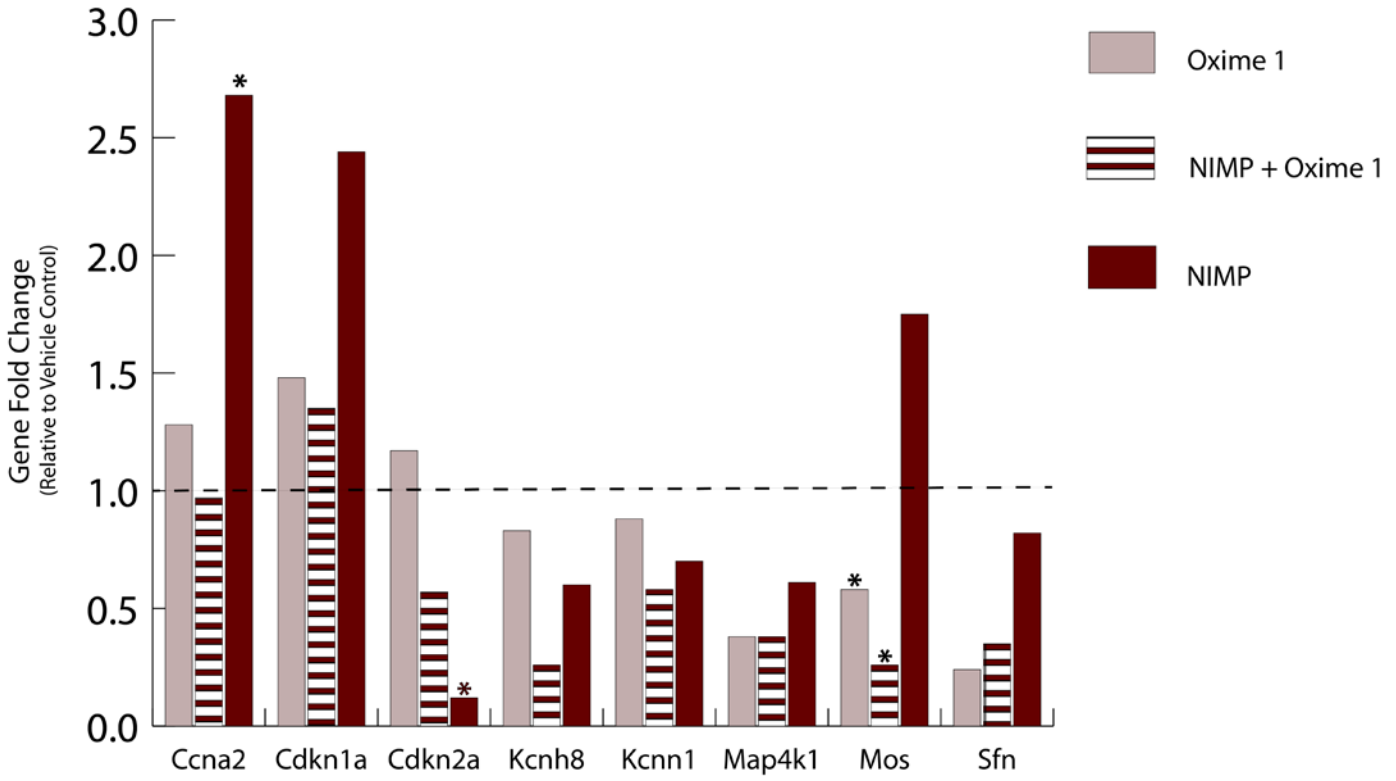

Figure 3.2 Fold Changes in Expression of Select MAP Kinase Genes by Treatment

Data on fold change of MAP kinase genes relative to vehicle control for all other treatments. Vehicle control value = 1.0. Fold change was calculated to represent normalized gene expression as (2^(- Delta Ct)).

CONCLUSION

With the significant toxicity and the widespread use of organophosphates in agriculture and potential for use in chemical warfare, these compounds pose a major public health concern. This is made even more concerning by the fact that there is not yet a treatment that is fully protective against central nervous system damage resulting from exposure to these chemicals. The novel pyridinium oximes developed by Dr. Howard Chambers have shown promise as potential therapeutics against organophosphate exposure, not only producing survival rates in animal models comparable to or better than 2-PAM but also reactivating inhibited AChE within the CNS and decreasing the duration of seizures. It is hoped that attenuation of seizure activity within the brain will prevent neuronal damage and the resulting mental alterations.

The results of the study described here are supportive of this theory that the novel oximes might be able to prevent organophosphate-induced neurodegeneration. Rats administered a lethal dose of paraoxon and treated with Oxime 20 had a lower incidence of neurodegeneration than rats receiving only paraoxon 24 hours after exposure. In rats perfused 4 days after this same exposure, no rat treated with Oxime 20 or Oxime 15 showed any sign of neural pathology while rats given only NIMP or paraoxon or paraoxon and 2-PAM stained positively for Fluoro-Jade B. These findings support that the novel oximes may be able to prevent excitotoxic neurodegeneration from OP exposure, which is an important component in treating OP exposure and preventing long-lasting cognitive impairment.

The molecular work from this study also explores the alterations in genomic regulation of the MAP kinase system as a result of both the nerve agent surrogate NIMP and Oxime 1. The ability of Oxime 1 to return changes in gene expression back towards baseline is supportive that this therapy is effective in attenuating organophosphate induced seizures. The changes that are seen in MAP kinase regulation as a result of NIMP treatment suggest that the primary effect of this OP with regards to MAP kinase is the induction of changes in the cell cycle. These changes have several interpretations as to their eventual outcome, but it is suggestive that the OP promotes apoptosis of the neurons of the piriform cortex. Oxime 1 alone produces changes in MAP kinase regulation that could lead to changes in neuronal excitability, neurotransmitter synthesis, apoptotic signaling, and cell cycle. The study of MAP kinase RNA regulation is an important area as this system controls various cellular responses to external stimuli. These findings support the concept that treatment with NIMP promotes apoptosis of cells within the central nervous system and that Oxime 1 attenuates this effect. The findings that Oxime 1 itself produces alterations of genomic expression are not fully unexpected but are of interest.

The model of OP exposure used in the Fluoro-Jade B study described here were proof of concept that both NIMP and paraoxon are capable of producing neurodegeneration in the rat model. Refinement of this model will likely be necessary in order to produce a higher incidence of neurodegeneration in test animals as currently only a small portion of those animals treated with the OPs developed neuropathology observable with Fluoro-Jade B. This makes attainment of statistical power difficult, as a high number of replications would be necessary to test for significance.

Future directions for these projects could be refinement of the OP exposure model to increase the rate at which animals show neurodegeneration, exploration of other biomarkers for observation of neuropathology that may be more sensitive to seizure induced stress, and further studies into the MAP kinase system such as protein phosphorylation, which may prove to be a better indicator of the activity within this system.

REFERENCES

Adamson, T. and N. Vasilyeva (2017). "France says analysis shows Syria regime behind sarin attack." ABCNews. Retrieved from abcnews.go.com.

Apland, J., T. Figueiredo, F. Qashu, V. Aroniadou-Anderjaska, A. Souza, and M. Braga (2010). "Higher susceptibility of the ventral versus the dorsal hippocampus and the posteroventral versus anterodorsal amygdala to soman-induced neuropathology." Neurotoxicology. 31(5):485-492.

Aranda, P., D. LaJoie, and C. Jorcyk (2012). "Bleach Gel: A Simple Agarose Gel for Analyzing RNA Quality." Electrophoresis. 33(2): 366–369.

Austin, L. and K. James (1970). "Rates of regeneration of acetylcholinesterase in rat brain subcellular fractions following DFP inhibition." J Neurochem. 17(5):705-707.

Baille, V., P. Clarke, G. Brochier, F. Dorandeu, J. Verna, E. Four, G. Lallement, and P. Carpentier (2005). "Soman-induced convulsions: The neuropathology revisited." Toxicology. 215(1-2):1-24.

Benton, D., A. Monghan, R. Hosseini, P. Bahia, D. Haylett, and G. Moss (2003). "Small conductance Ca2+-activated K+ channels formed by the expression of rat SK1 and SK2 genes in HEK 293 cells." J Physiol. 553(1):13-19.

Bhat, R., E. Crowe, A. Bitto, M. Moh, C. Katsetos, F. Garcia, F. Johnson, J. Trojanowski, C. Sell, and C. Torres (2012). "Astrocyte senescence as a component of Alzheimer's disease." PLoS One. 7(9).

Blanton, J., J. D'Ambrozio, J. Sistrunk, and E. Midboe (2004). "Global Changes in the Expression Patterns of RNA Isolated from the Hippocampus and Cortex of VX Exposed Mice." J Biochem Mol Toxicol. 18(3):115-123.

Bostrom, J., B. Meyer-Puttlitz, M. Wolter, B. Blaschke, R. Weber, P. Lichter, K. Ichimura, V. Collins, and G. Reifenberger (2001). "Alterations of the Tumor Suppressor Genes CDKN2A ($p16^{INK4a}$), $p14^{ARF}$, CDKN2B ($p15^{INK4b}$), and CDKN2C ($p18^{INK4c}$) in Atypical and Anaplastic Meningiomas." Am J Pathol. 159(2):661–669.

Brown, J. and P. Taylor (2006). Muscarinic Receptor Agonists and Antagonists. In Brunton, L., J. Lazo, and K. Parker (Eds.). *Goodman & Gilman's The Pharmacological Basis of Therapeutics*. New York: The McGraw Hill Companies.

Cazzalini, O., A. Scovassi, M. Savio, L. Stivala, and E. Prosperi (2010). "Multiple roles of the cell cycle inhibitor $p21^{CDKN1A}$ in the DNA damage response." Mutat Res. 704(1-3):12-20.

Chambers, J., H. Chambers, E. Meek, and R Pringle (2013). "Testing of novel brain-penetrating oxime reactivators of acetylcholinesterase inhibited by nerve agent surrogates."Chemico-Biological Interactions. 203(1):135-138.

Chambers, J., E. Meek, J. Bennett, W. Bennett, H. Chambers, C. Leach, R. Pringle and R. Wills (2016). "Novel substituted phenoxyalkyl pyridinium oximes enhance survival and attenuate seizure-like behavior of rats receiving lethal levels of nerve agent surrogates." Toxicology. 339:51-57.

Chapman, S., T. Kadar, and E. Gilat (2007). "Seizure duration following sarin exposure affects neuro-inflammatory markers in the rat brain." Neurotoxicology. 27(2):277-283.

Chen, Y. and R. Swanson (2003). "Review Article: Astrocytes and Brain Injury." J Cereb Blood Flow Metab. 23(2):137-149.

Chen, Y. (2012). "Organophosphate-induced brain damage: Mechanisms, neuropsychiatric and neurological consequences, and potential therapeutic strategies." Neurotoxicology. 33(3):391-400.

Collombet, J., E. Four, W. Fauquette, M. Burckhart, C. Masqueliez, D. Bernabe, D. Baubichon, and G. Lallement (2007). "Soman poisoning induces delayed astrogliotic scar and angiogenesis in damaged mouse brain areas." Neurotoxicology. 28(1):38-48.

Collombet, J., D. Beracochea, P. Liscia, C. Pierard, G. Lallement, and P. Filliat (2011). "Long-term effects of cytokine treatment on cognitive behavioral recovery and neuronal regeneration in soman-poisoned mice." Behav Brain Res. 221(1):261-270.

Costa, L (2008). Toxic Effects of Pesticides. In Klaassen, C. (Ed.). *Casarett & Doull's Toxicology: The Basic Science of Poisons*. New York: The McGraw Hill Companies.

Damodaran, T., A. Patel, S. Greenfield, H. Dressman, S. Lin, and M. Abou-Donia (2006). "Gene expression profiles of the rat brain both immediately and 3 months following acute sarin exposure." Biochem Pharmacol. 71(4):497-520.

Deng, J., G. Gao, L. Wang, T. Wang, J. Yu, and Z. Zhao (2011). "Stratifin expression is a novel prognostic factor in human gliomas." Pathol Res Pract. 207(11):674-679.

Deshpande, L., D. Carter, R. Blair, and R. DeLorenzo (2010). "Development of a Prolonged Calcium Plateau in Hippocampal Neurons in Rats Surviving Status Epilepticus Induced by the Organophosphate Diisopropylfluorophosphate." Toxicol Sci. 116(2):623-631.

Deshpande, L., K. Phillips, B. Huang, and R. DeLorenzo (2014a). "Chronic behavioral and cognitive deficits in a rat survival model of paraoxon toxicity." Neurotoxicology. 44:352-357.

Deshpande, L., D. Carter, K. Phillips, R. Blair, and R. DeLorenzo (2014b). "Development of status epilepticus, sustained calcium elevations and neuronal injury in a rat survival model of lethal paraoxon intoxication." Neurotoxicology. 44:17-26.

Deshpande, L., R. Blair, B. Huang, K. Phillips, and R. DeLorenzo (2016a). "Pharmacological blockade of the calcium plateau provides neuroprotection following organophosphate paraoxon induced status epilepticus in rats." Neurotoxicol Teratol. 56:81-86.

Deshpande, L., R. Blair, K. Phillips, and R. DeLorenzo (2016b). "Role of the calcium plateau in neuronal injury and behavioral morbidities following organophosphate intoxication." Ann N Y Acad Sci. 1374(1):176-183.

D'hoedt, D., K. Hirzel, P. Pedarzani, and M. Stocker (2004). "Domain analysis of the calcium-activated potassium channel SK1 from rat brain. Functional expression and toxin sensitivity." J Biol Chem. 279(13):12088-12092.

Dikovskaya, D., J. Cole, S. Mason, C. Nixon, S. Karim, L. McGarry, W. Clark, R. Hewitt, M. Sammons, J. Zhu, D. Athineos, J. Leach, F. Marchesi, J. van Tuyn, S. Tait, C. Brock, J. Morton, H. Wu, S. Berger, K. Blyth, and P. Adams (2015). "Mitotic Stress Is an Integral Part of the Oncogene-Induced Senescence Program that Promotes Multinucleation and Cell Cycle Arrest." Cell Rep. 12(9):1483-1496.

Dillman, J., C. Phillips, D. Kniffin, C. Tompkins, T. Hamilton, and R. Kan (2009). "Gene Expression Profiling of Rat Hippocampus Following Exposure to the Acetylcholinesterase Inhibitor Soman." Chem Res Toxicol. 22(4):633-638.

Eisenkraft, A., A. Falk, and A. Finkelstein (2013). "The Role of Glutamate and the Immune System in Organophosphate-induced CNS Damage." Neurotox Res. 24(2):265-279.

Ellwardt E., J. Walsh, J. Kipnis, and F. Zipp (2016). "Understanding the Role of T Cells in CNS Homeostasis." Trends Immunol. 37(2):154-65.

Ferl, R., M. Manak, and M. Reyer (2002). "The 14-3-3s." Genome Biol. 3(7).

Ferreira, W., M. Araujo, N. Anselmo, E. Oliveira, J. Brito, R. Burbano, M. Harada, and B. Borger (2015). "Expression Analysis of Genes Involved in the RB/E2F Pathway in Astrocytic Tumors." PLoS One. 10(8).

Filliat, P., S. Coubard, C. Pierard, P. Liscia, D. Beracochea, E. Four, D. Baubichon, C. Masqueliez, G. Lallement, and J. Collombet (2007). "Long-term behavioral consequences of soman poisoning in mice." Neurotoxicology. 28(3):508-519.

Finkelstein, A., G. Kunis, T. Berkutzki, A. Ronen, A. Krivoy, E. Yoles, D. Last, Y. Mardor, K. Shura, E. McFarland, B. Capacio, C. Eisner, M. Gonzales, D. Gregorowicz, A. Eisenkraft, J. McDonough, and M. Schwartz (2012). "Immunomodulation by poly-YE reduces organophosphate-induced brain damage." Brain Behav Immun. 26(1):159-169.

Fukuto, T. and R. Metcalf (1958). "The Effect of Structure on the Reactivity of Alkylphosphonate Esters." J. Am. Chem. Soc. 81(2): 372–377.

Fung, T., H. Ma, and R. Poon (2007). "Specialized Roles of the Two Mitotic Cyclins in Somatic Cells: Cyclin A as an Activator of M Phase–promoting Factor." Mol Biol Cell. 18(5):1861-1873.

Furukawa, A., Y. Kawamoto, Y. Chiba, S. Takei, S. Hasegawa-Ishii, N. Kawamura, K. Yoshikawa, M. Hosokawa, S. Oikawa, M. Kato, and A. Shimada (2011). "Proteomic identification of hippocampal proteins vulnerable to oxidative stress in excitotoxin-induced acute neuronal injury." Neurobiol Dis. 43(3):706-714.

Gage, G., D. Kipke, and W. Shain (2012). "Whole Animal Perfusion Fixation for Rodents." J Vis Exp. (65).

Gallo, M. and N. Lawryk (1991). Organic Phosphorus Pesticides. In Hayes W. and E. Laws (Eds.). *Handbook of Pesticide Toxicology*. San Diego: Academic Press.

Giorgi, F., M. Ferrucci, G. Lazzeri, C. Pizzanelli, P. Lenzi, M. Alessandri, L. Murri, and F. Fornai (2003). "A damage to locus coeruleus neurons converts sporadic seizures into self-sustaining limbic status epilepticus." Eur J Neurosci. 17(12):2593-2601.

Golden, G., G. Smith, T. Ferraro, and P. Reyes (1995). “Rat strain and age differences in kainic acid induced seizures.” Epilepsy Res. 20(2):151-159.

Goncalves, A., E. Cortesao, B. Oliveiros, V. Alves, A. Espadana, L. Rito, E. Magalhaes, S. Pereira, A. Pereira, J. Costa, L. Mota-Vieira, and B. Sarmento-Ribeiro (2016). “Oxidative stress levels are correlated with P15 and P16 gene promoter methylation in myelodysplastic syndrome patients.” Clin Exp Med. 16(3):333-343.

Gonzalez-Garcia, J., J. Bradley, M. Nomikos, L. Paul, Z. Machaty, F. Lai, and K. Swann (2014). “The dynamics of MAPK inactivation at fertilization in mouse eggs.” J Cell Sci. 127(12):2749-2760.

Gygli, P., J. Chang, H. Gokozan, F. Catacutan, T. Schmidt, B. Kaya, M. Goksel, F. Baig, S. Chen, A. Griveau, W. Michowski, M. Wong, K. Palanichamy, P. Sicinski, R. Nelson, C. Czeisler, and J. Otero (2016). “Cyclin A2 promotes DNA repair in the brain during both development and aging.” Aging 8(7):1540-1570.

Hermeking, H., C. Lengauer, K. Polyak, T. He, L. Zhang, S. Thiagalingam, K. Kinzler, and B. Vogelstein (1997). “14-3-3r Is a p53-Regulated Inhibitor of G2/M Progression.” Mol Cell. 1(1):3-11.

Hermeking, H. (2004). “Extracellular 14-3-3sigma protein: a potential mediator of epithelial-mesenchymal interactions.” J Invest Dermatol. 124(1):ix-x.

Hommes, D,. M. Peppelenbosch, and S. van Deventer (2003). “Mitogen activated protein (MAP) kinase signal transduction pathways and novel anti-inflammatory targets.” Gut. 52(1):144-151.

Kalejs, M., A. Ivanov, G. Plakhins, M. Cragg, D. Emzinsh, T. Illidge, and J. Erenpreisa (2006). “Upregulation of meiosis-specific genes in lymphoma cell lines following genotoxic insult and induction of mitotic catastrophe.” BMC Cancer. 6:6.

Katchanov, J., C. Harms, K. Gertz, L. Hauck, C. Waeber, L. Hirt, J. Priller, R. von Harsdorf, W. Bruck, H. Hortnagl, U. Dirnagl, P. Bhide, and M. Endres (2001). “Mild Cerebral Ischemia Induces Loss of Cyclin-Dependent Kinase Inhibitors and Activation of Cell Cycle Machinery before Delayed Neuronal Cell Death.” J Neurosci. 21(14):5045-5053.

Kawauchi, T., M. Shikanai, and Y. Kosodo (2013). “Extra-cell cycle regulatory functions of cyclin-dependent kinases (CDK) and CDK inhibitor proteins contribute to brain development and neurological disorders.” Genes Cells. 18(3):176-194.

Kim, A., G. Khursigara, X. Sun, T. Franke, and M. Chao (2001). "Akt Phosphorylates and Negatively Regulates Apoptosis Signal-Regulating Kinase 1." Mol Cell Biol. 21(3):893-901.

Krishnan, J., P. Arun, A. Appu, N. Vijayakumar, T. Figueiredo, M. Braga, S. Baskota, C. Olsen, N. Farkas, J. Dagata, W. Frey, J. Moffett, and A. Namboodiri (2016). "Intranasal delivery of obidoxime to the brain prevents mortality and CNS damage from organophosphate poisoning." Neurotoxicology. 53:64-73.

Lallement, G., P. Carpentier, A. Collet, I. Pernot-Marino, D. Baubichon, and G. Blanchet (1991). "Effects of soman-induced seizures on different extracellular amino acid levels and on glutamate uptake in rat hippocampus." Brain Res. 563(1-2):234-240.

Lasserre, R., C. Cuche, R. Blecher-Gonen, E. Libman, E. Biquand, A. Danckaert, D. Yablonski, A. Alcover, and V. Bartolo (2011). "Release of serine/threonine-phosphorylated adaptors from signaling microclusters down-regulates T cell activation." J Cell Biol. 195(5):839-853.

Li, T., D. Han, J. Chen, X. Yu, and G. Zhang (2008a). "Neuroprotection against ischemic brain injury by knockdown of hematopietic progenitor kinase 1 expression." Neuroreport. 19(6):647-651.

Li, T., X. Yu, and G. Zhang (2008b). "Tyrosine phosphorylation of HPK1 by activated Src promotes ischemic brain injury in rat hippocampal CA1 region." FEBS Lett. 582(13):1894-1900.

Li, Z., J. Liu, and J. Zhang (2009). "14-3-3σ, the double-edged sword of human cancers" Am J Transl Res. 1(4):326-340.

Li, Y., P. Lein, C. Liu, D. Bruun, T. Tewolde, G. Ford, and B. Ford (2011). "Spatiotemporal pattern of neuronal injury induced by DFP in rats: A model for delayed neuronal cell death following acute OP intoxication." Toxicol Appl Pharmacol. (3):261-269.

Liu, S., W. Bishop, and M. Liu (2003). "Differential effects of cell cycle regulatory protein $p21^{WAF1/Cip1}$ on apoptosis and sensitivity to cancer chemotherapy." Drug Resist Updat. 6(4):183-195.

Loukil, A., F. Izard, M. Georgieva, S. Mashayekhan, J. Blanchard, A. Parmeggiani, and M. Peter (2016). "Foci of cyclin A2 interact with actin and RhoA in mitosis." Sci Rep. 6:27215.

Loveluck, L. (2017). "Sarin was used in deadly Syria attack, chemical weapons watchdog confirms." The Washington Post. Retrived from www.washingtonpost.com.

Masson, P. (2011). “Evolution of and perspectives on therapeutic approaches to nerve agent poisoning.” Toxicol Lett. 206(1):5-13.

McDonough, J., N. Jaax, R. Crowley, M. May, and H. Modrow (1989). “Atropine and/or diazepam therapy protects against soman-induced neural and cardiac pathology.” Fundam Appl Toxicol. 13(2):256-276.

McDonough, J., L. Dochterman, C. Smith, and T. Shih (1995). “Protection Against Nerve Agent-Induced Neuropathology, But Not Cardiac Pathology, is Associated with the Anticonvulsant Action of Drug Treatment.” Neurotoxicology. 16(1):123-132.

McDonough, J., L. Zoeffel, J. McMonagle, T. Copeland, C. Smith, and T. Shih (2000). “Anticonvulsant treatment of nerve agent seizures: anticholinergics versus diazepam in soman-intoxicated guinea pigs.” Epilepsy Res. 38(1):1-14.

Mebratu, Y. and Y. Tesfaigzi (2009). “How ERK1/2 Activation Controls Cell Proliferation and Cell Death Is Subcellular Localization the Answer?.” Cell Cycle. 8(8):1168-1175.

Meek, E., H. Chambers, A. Coban, K. Funck, R. Pringle, M. Ross, and J. Chambers (2012). “Synthesis and In Vitro and In Vivo Inhibition Potencies of Highly Relevant Nerve Agent Surrogates.” Toxicol Sci. 126(2):525-533.

Motte, J., M. Fernandes, T. Baram, and A. Nehlig (1998). “Spatial and temporal evolution of neuronal activation, stress and injury in lithium-pilocarpine seizures in adult rats.” Brain Res. 793(1-2):61-72.

Myhrer, T., J. Andersen, N. Nguyen, and P. Aas (2005). “Soman-induced Convulsions in Rats Terminated with Pharmacological Agents after 45 min: Neuropathology and Cognitive Performance.” Neurotoxicology. 26(1):39-48.

Myhrer, T., S. Enger, and P. Aas (2006). “Efficacy of Immediate and Subsequent Therapies against Soman-Induced Seizures and Lethality in Rats.” Basic Clin Pharmacol Toxicol. 98(2):184-191.

Nagao, M., K. Campbell, K. Burns, C. Kuan, A. Trumpp, and M. Nakafuku (2008). “Coordinated control of self-renewal and differentiation of neural stem cells by Myc and the $p19^{ARF}$–p53 pathway.” J Cell Biol. 183(7):1243-1257.

Niijima, H., M. Nagao, M. Nakajima, T. Takatori, M. Iwasa, Y. Maeno, H. Koyama, and I. Isobe (2000). “The effects of sarin-like and soman-like organophosphorus agents on MAPK and JNK in rat brains.” Forensic Sci Int. 112(2-3):171-178.

Norwood, B., S. Bauer, S. Wegner, H. Hamer, W. Oertel, R. Sloviter, and F. Rosenow (2011). “Electrical stimulation-induced seizures in rats: a "dose-response" study on resultant neurodegeneration.” Epilepsia. 52(9):109-112.

Ohta, H., T. Ohmori, S. Suzuki, H. Ikegaya, K. Sakurada, and T. Takatori (2006). “New safe method for preparation of sarin-exposed human erythrocytes acetylcholinesterase using non-toxic and stable sarin analogue isopropyl p-nitrophenyl methylphosphonate and its application to evaluation of nerve agent antidotes.” Pharm Res. 23(12):2827-2833.

Paxinos, G. and C. Watson (2006). *The Rat Brain in Stereotaxic Coordinates 6th Edition*. London: Academic Press.

Perrard, M., E. Chassaing, G. Montillet, O. Sabido, and P. Durand (2009). “Cytostatic Factor Proteins Are Present in Male Meiotic Cells and b-Nerve Growth Factor Increases Mos Levels in Rat Late Spermatocytes.” PLoS One. 4(10).

Qiagen (2011). *RT2 Profiler PCR Array (96-Well Format and 384-Well [4 x 96] Format) Rat MAP Kinase Signaling Pathway*. Valencia, CA.

RamaRao, G., C. Waghmare, N. Srivastava, and B. Bhattacharya (2010). “Regional alterations of JNK3 and CaMKIIα subunit expression in the rat brain after soman poisoning.” Hum Exp Toxicol. 30(6):448-459.

RamaRao, G., P. Afley, J. Acharya, and B. Bhattacharya (2014). “Efficacy of antidotes (midazolam, atropine and HI-6) on nerve agent induced molecular and neuropathological changes.” BMC Neurosci. 15:47.

Roninson, I. (2002). “Oncogenic functions of tumour suppressor $p21^{Waf1/Cip1/Sdi1}$: association with cell senescence and tumour-promoting activities of stromal fibroblasts.” Cancer Lett. 179(1):1-14.

Saganich, M., E. Machado, and B. Rudy (2001). “Differential expression of genes encoding subthreshold-operating voltage-gated K+ channels in brain.” J Neurosci. 2001 21(13):4609-4624.

Schmued, L., C. Albertson, and W. Slikker (1997). “Fluoro-Jade: a novel fluorochrome for the sensitive and reliable histochemical localization of neuronal degeneration.” Brain Res. 751(1):37-46.

Schmued, L. and K. Hopkins (2000). “Fluoro-Jade B: a high affinity fluorescent marker for the localization of neuronal degeneration.” Brain Res. 874(2):123-130.

Schneider, C., W. Rasband, and K. Eliceiri (2012). "NIH Image to ImageJ: 25 years of image analysis", Nature methods. 9(7): 671-675.

Seidel, K., S. Kirsch, K. Lucht, D. Zaade, J. Reinemund, J. Schmitz, S. Klare, Y. Li, J. Schefe, K. Schmerbach, P. Goldin-Lang, F. Zollmann, C. Thone-Reineke, T. Unger, and H. Funke-Kaiser (2011). "The Promyelocytic Leukemia Zinc Finger (PLZF) Protein Exerts Neuroprotective Effects in Neuronal Cells and is Dysregulated in Experimental Stroke." Brain Pathol. 21(1):31-43.

Serrano, M., G. Hannon, and D. Beach (1993). "A new regulatory motif in cell-cycle control causing specific inhibition of cyclin D/CDK4." Nature. 366(6456):704-707.

Shih, T. and J. McDonough (1997). "Neurochemical Mechanisms in Soman-induced Seizures." J Appl Toxicol. 17(4):255-264.

Shih, T., S. Duniho, and J. McDonough (2003). "Control of nerve agent-induced seizures is critical for neuroprotection and survival." Toxicol Appl Pharmacol. 188(2):69-80.

Simoni, M., C. Perego, T. Ravizza, D. Moneta, M. Conti, F. Marchesi, A. De Luigi, S. Garattini, and A. Vezzani (2000). "Inflammatory cytokines and related genes are induced in the rat hippocampus by limbic status epilepticus." Eur J Neurosci. 12(7):2623-2633.

Siso, S., B. Hobson, D. Harvey, D. Bruun, D. Rowland, J. Garbow, and P. Lein (2017). "Spatiotemporal Progression and Remission of Lesions in the Rat Brain Following Acute Intoxication With Diisopropylfluorophosphate." Toxicol Sci. 157(2):330-341.

Soltaninejad, K. and S. Shadnia (2014). History of the Use and Epidemiology of Organophosphorus Poisoning. In Balali-Mood and Abdollahi (Eds.), *Basic and Clinical Toxicology of Organophosphorus Compounds.* London: Springer-Verlag.

Spradling, K., L. Lumley, C. Robison, J. Meyerhoff, and J. Dillman (2011). "Transcriptional analysis of rat piriform cortex following exposure to the organophosphonate anticholinesterase sarin and induction of seizures." J Neuroinflammation. 8:83.

Tam, K., W. Zhang, J. Soh, V. Stastny, M. Chen, H. Sun, K. Thu, J. Rios, C. Yang, C. Marconett, S. Selamat, I. Laird-Offringa, A. Taguchi, S. Hanash, D. Shames, X. Ma, M. Zhang, W. Lam, and A. Gazdar (2013). "CDKN2A/p16 Inactivation Mechanisms and Their Relationship to Smoke Exposure and Molecular Features in Non–Small-Cell Lung Cancer." J Thorac Oncol. 8(11):1378-1388.

Tane, S. and T. Chibazakura (2009). "Cyclin A overexpression induces chromosomal double-strand breaks in mammalian cells." Cell Cycle. 8(23):3900-3903.

Te, J., K. Spradling-Reeves, J. Dillman, and A. Wallqvist (2015). "Neuroprotective mechanisms activated in non-seizing rats exposed to sarin." Brain Res. 1618:136-148.

U. S. Environmental Protection Agency/Office of Chemical Safety and Pollution Prevention (2011). *Pesticides Industry Sales and Usage: 2006 and 2007 Market Estimates.* Washington, DC: Grube, A., D. Donaldson, T. Kiely, and L. Wu.

Wang, Y., L. Qu, X. Wang, L. Gao, Z. Li, G. Gao, and Q. Yang (2015). "Firing pattern modulation through SK channel current increase underlies neuronal survival in an organotypic slice model of Parkinson's disease." Mol Neurobiol. 51(1):424-436.

Watson, A., D. Opresko, R. Young, V. Hauschild, J. King, and K. Bakshi (2009). Organophosphate Nerve Agents. In Gupta, R. (Ed.). *Handbook of Toxicology of Chemical Warfare Agents.* London: Academic Press.

Wu, J., Z. Zhao, B. Sabirzhanov, B. Stoica, A. Kumar, T. Luo, J. Skovira, and A. Faden (2014). "Spinal Cord Injury Causes Brain Inflammation Associated with Cognitive and Affective Changes: Role of Cell Cycle Pathways." J Neurosci. 34(33):10989-11006.

Zhao, R., B. Choi, M. Lee, A. Bode, and Z. Dong (2016). "Implications of Genetic and Epigenetic Alterations of CDKN2A ($p16^{INK4a}$) in Cancer." EBioMedicine. 8:30-39.

Zimmer, L., M. Ennis, and M. Shipley (1997). "Soman-Induced Seizures Rapidly Activate Astrocytes and Microglia in Discrete Brain Regions." BMC Neurosci. 15:47.